Competition between Superconductivity and Localization across the Disorder-Driven Superconductor-Insulator quantum phase transition

Institute of Semiconductor Physics, Novosibirsk, Russia
Tatyana Baturina

A. I. LARKIN MEMORIAL CONFERENCE
June 24-28, 2007,
Chernogolovka, Russia

Outline

✓ Suppression of Superconductivity by Disorder

- Superconductor – Metal – Insulator transition (SMIT)
- Superconductor – Insulator transition (SIT)

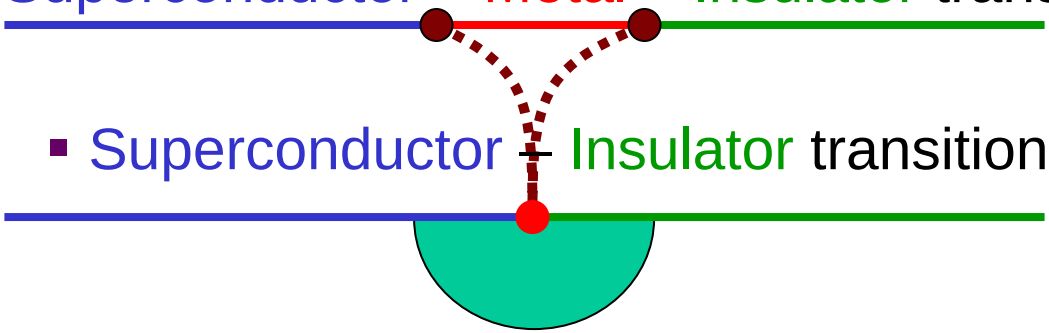

Main focus: **Critical Region of the Disorder-Driven Superconductor-Insulator quantum phase transition**

✓ the response to applied magnetic and/or electric fields

picture-gallery

“In search of disorder-driven superconductor-insulator transition”

***** collection *****

Suppression of Superconductivity by Disorder

D.V. Haviland, Y. Liu, and A.M. Goldman,
PRL **62**, 2180 (1989)

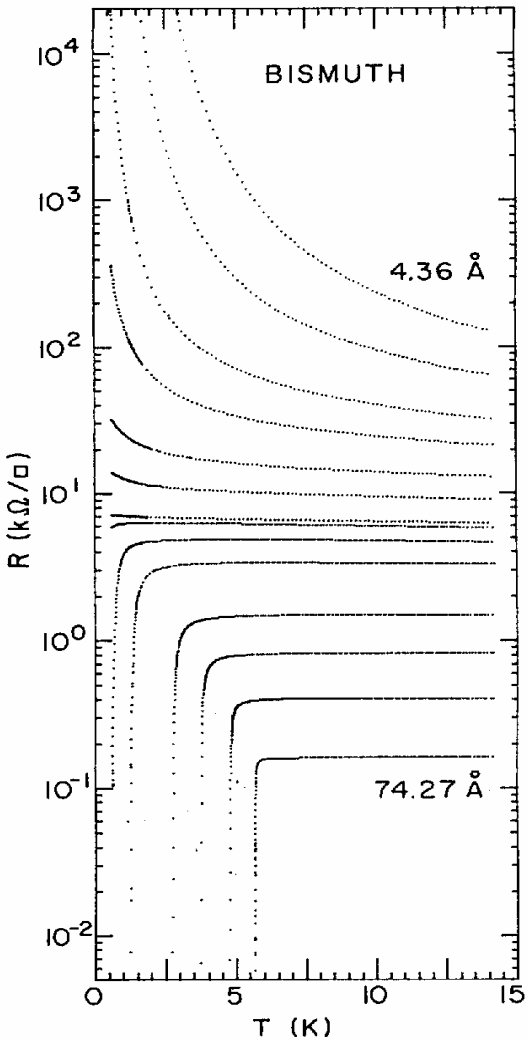

$d < d_c$ Insulator

d_c Metal

$d > d_c$ Superconductor

Bi films
$R_c = 6.45\ k\Omega$

$R_c = h/(2e)^2$

Fan-shaped curves

The onset of superconductivity in homogeneous ultrathin films is found to occur when their normal-state sheet resistance falls below a value close to $h/4e^2$, the quantum resistance for pairs. The data fur-

Suppression of Superconductivity by Disorder

Bi films R_c = 6.45 kΩ

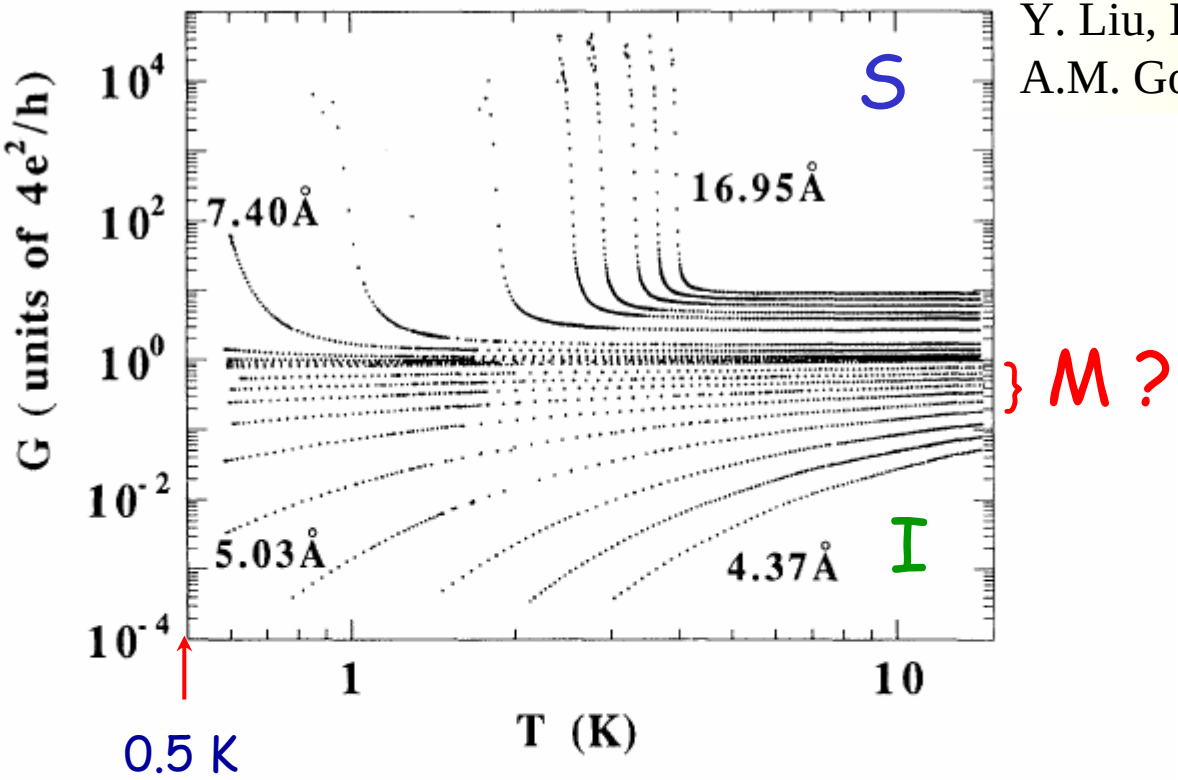

Y. Liu, D.V. Haviland, B. Nease, and A.M. Goldman, PRB **47**, 5931 (1993)

FIG. 2. Evolution for Bi films of the electrical conductance G in units of $4e^2/h$ as a function of temperature T. The thicknesses of a few selected films are indicated. Note that conductance and conductivity are identical in two dimensions. Only some of the data of the sequence of films is shown to avoid too high a density of data points.

Suppression of Superconductivity by Disorder

Bi films

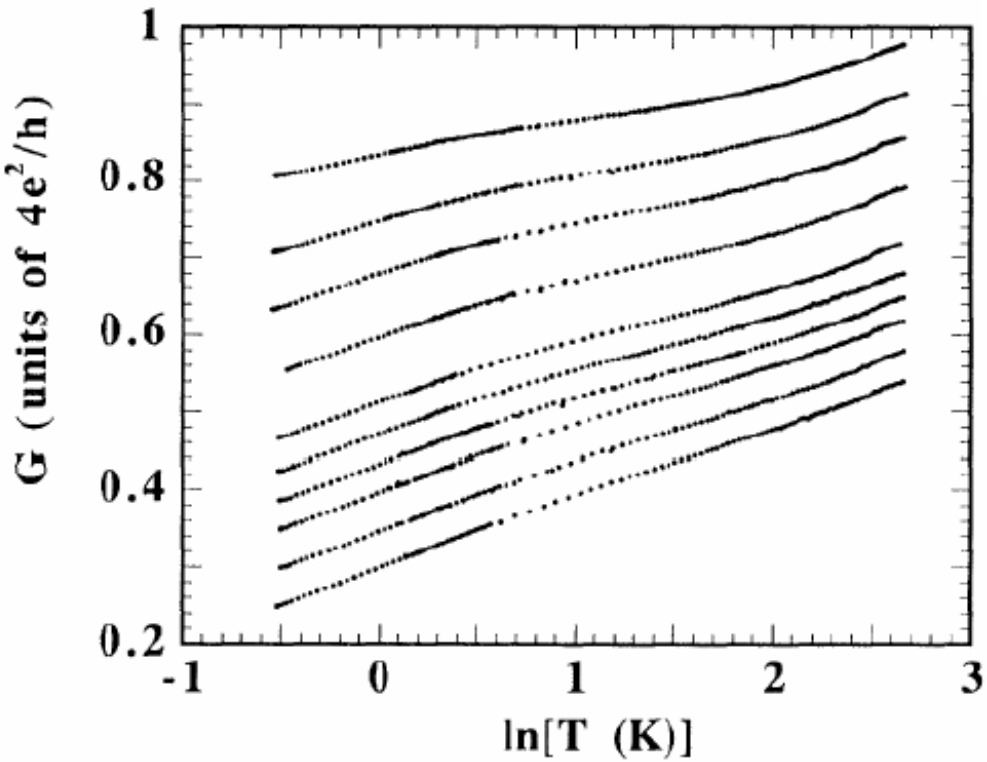

Y. Liu, D.V. Haviland, B. Nease, and A.M. Goldman, PRB **47**, 5931 (1993)

$G \propto \ln T$

} M ?

metal

Drude conductivity

+

quantum corrections

FIG. 6. Conductance G vs $\ln T$ of last ten insulating Bi films. (The 22nd to 31st films of the Bi sequence.) The temperature dependences of the conductances are approximately logarithmic. Notice that in the low-temperature limit, the slope of the logarithm decreases as the onset of superconductivity is approached.

SMIT

Suppression of Superconductivity by Disorder

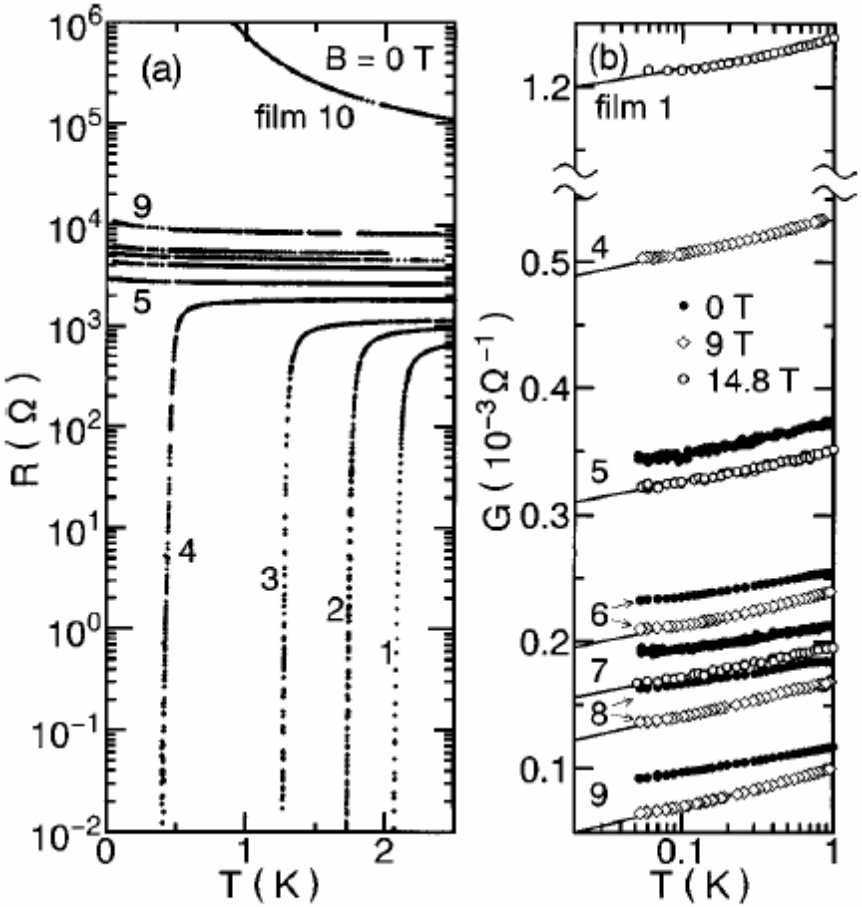

Mo_xSi_{1-x} films

S. Okuma, T. Terashima, and Kokubo, PRB 58, 2816 (1998).

$G \propto \ln T$

metal

Drude conductivity

+

quantum corrections

SMIT

Figure 1(a) illustrates the temperature dependence of the sheet resistance $R(T)$ in $B=0$ for ten selected films. Films with $R_n(10\ \mathrm{K})$ smaller than 1.8 kΩ (films 1–4) achieve global superconductivity, while those with $R_n(10\ \mathrm{K})$ larger than 2.5 kΩ (films 5–10) behave like an insulator, showing an increase in R at low temperatures.

Ta films

Y. Qin, C.L. Vicente, J. Yoon,
PRB 73, 100505(R) (2006).

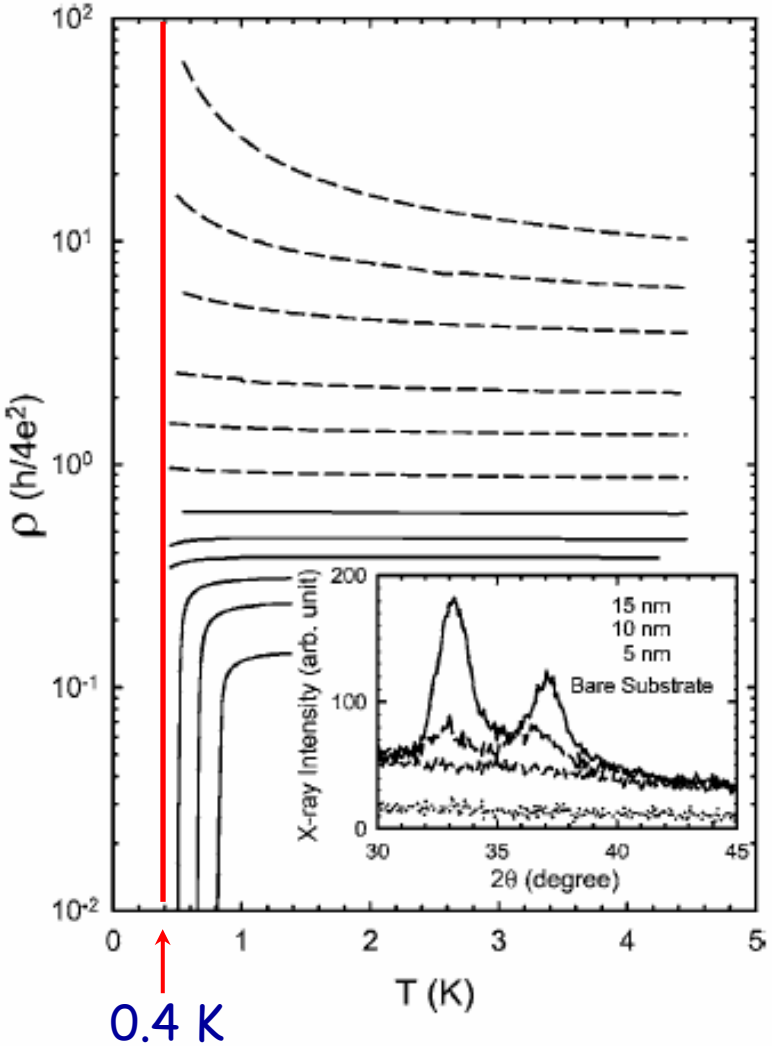

← 6.45 kΩ

SMIT ?

or
additional study
at lower temperature
is needed

FIG. 1. The resistance is measured at $B=0$ with a dc current in the range 1–10 nA that is within the linear response regime. The thicknesses of the films are, from the top, 1.9, 2.0, 2.1, 2.3, 2.5, 2.8, 3.1, 3.4, 3.7, 4.0, 4.5, and 5.5 nm. The dashed lines are for the insulating phase and the solid lines are for the superconducting phase. Inset: x-ray diffraction patterns of 15, 10, 5 nm thick Ta films, and a bare Si substrate.

InO_x films

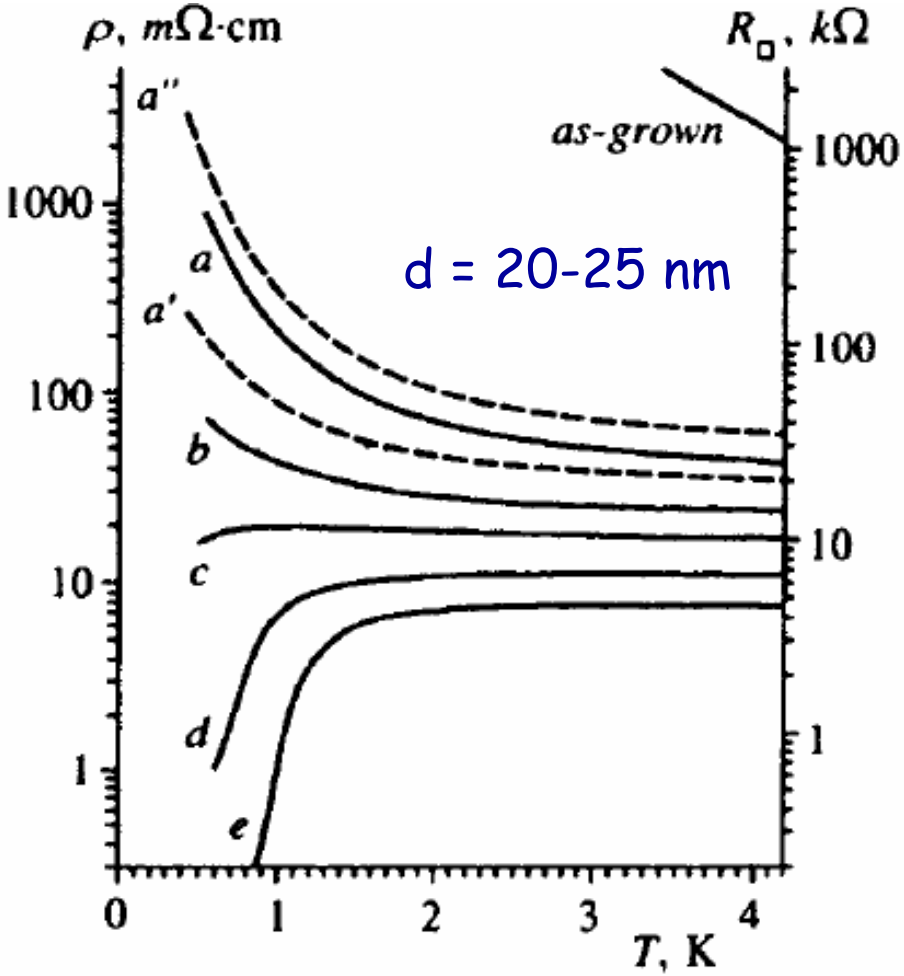

V.F. Gantmakher *et al.*, JETP 82, 951 (1996).

FIG. 2. Evolution of the temperature dependence of the resistance of a-In_2O_x films in zero magnetic field after different treatments. Film No. 1: states a (initial)–e, film No. 2: states a' (initial) and a''. A part of the dependence $R(T)$ for the as-grown film from the inset of Fig. 1 is also plotted.

Be films

E. Bielejec, J. Ruan, and W. Wu
PRL 87, 36801 (2001).

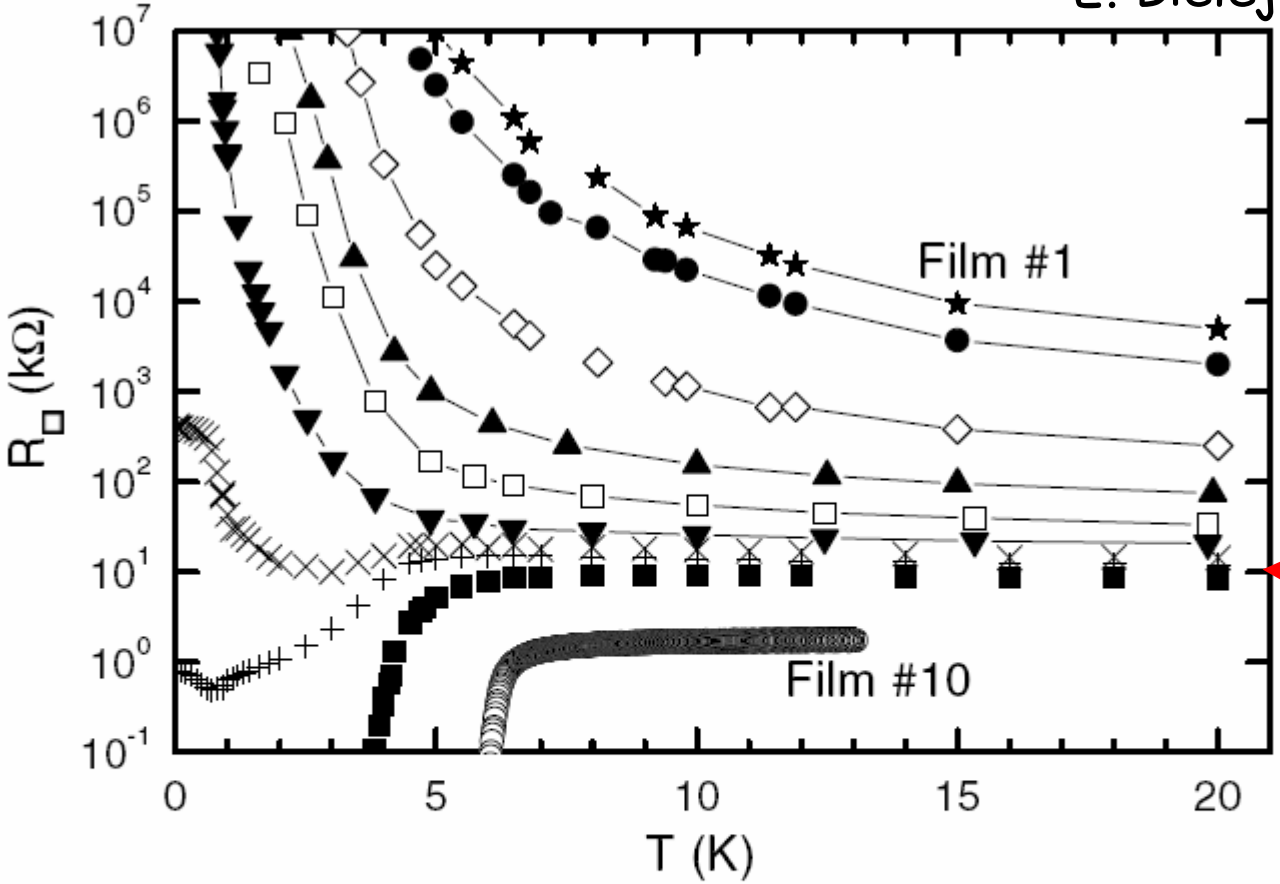

$R_c \approx 10\ k\Omega$

FIG. 1. Curves of film sheet resistance as a function of temperature measured on one film section following a series of deposition steps to increase film thickness. For curves from top to bottom, we label them as Film #1 to Film #10, respectively. The thickness for these films changed from 4.6 to 15.5 Å.

Experiment TiN films

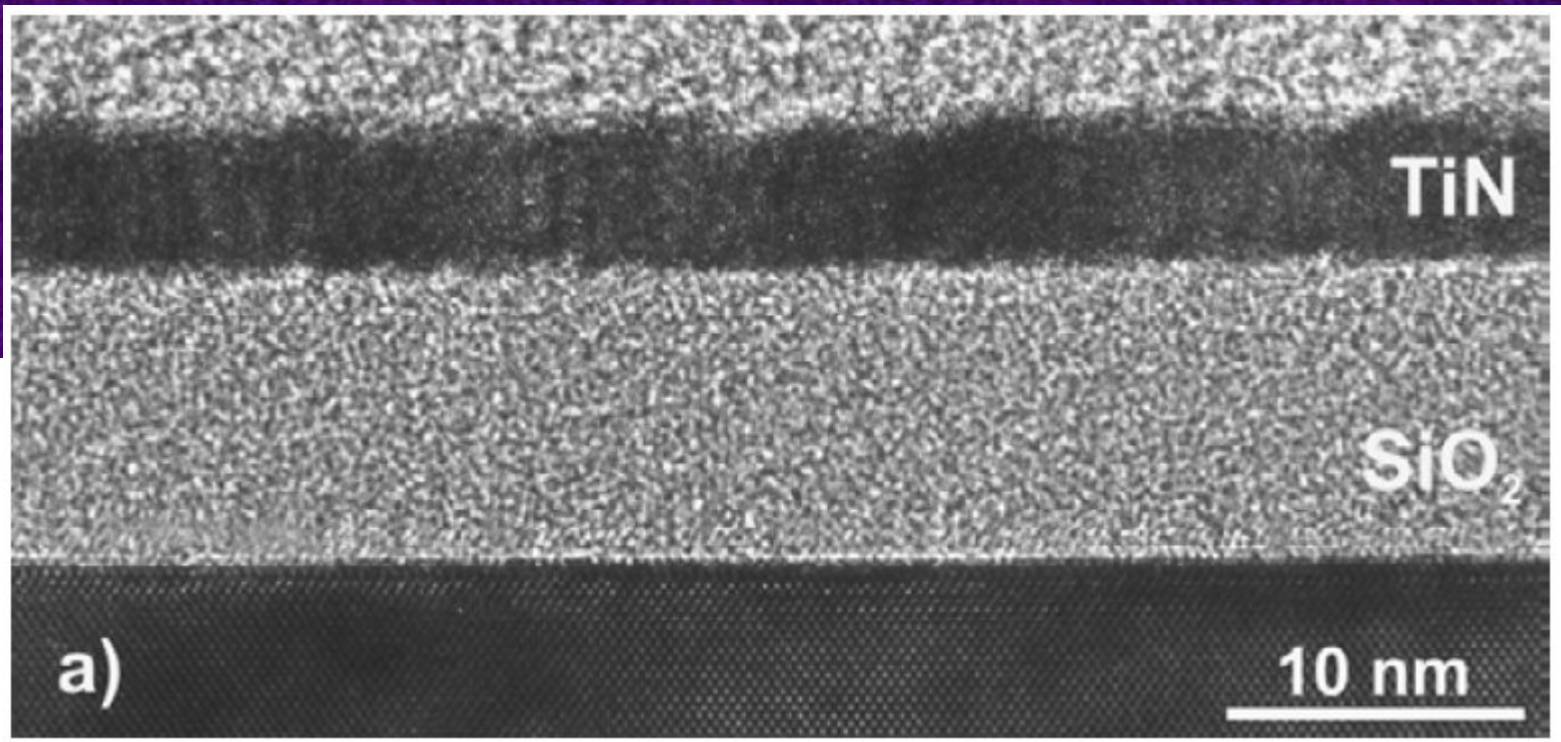

✓ TiN films were formed by atomic layer chemical vapor deposition onto a Si/SiO_2 substrate.

d = 5 nm

TiN films

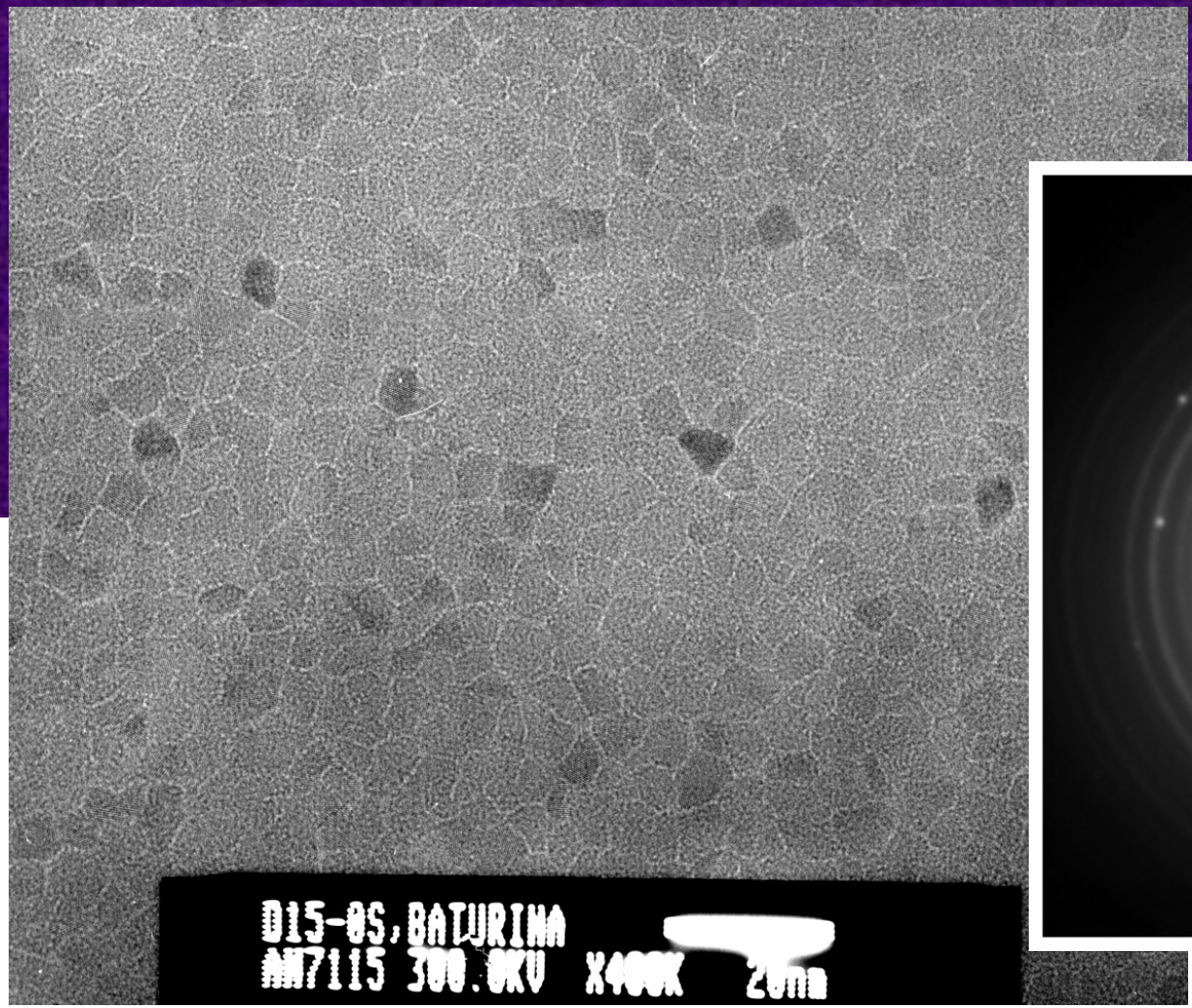

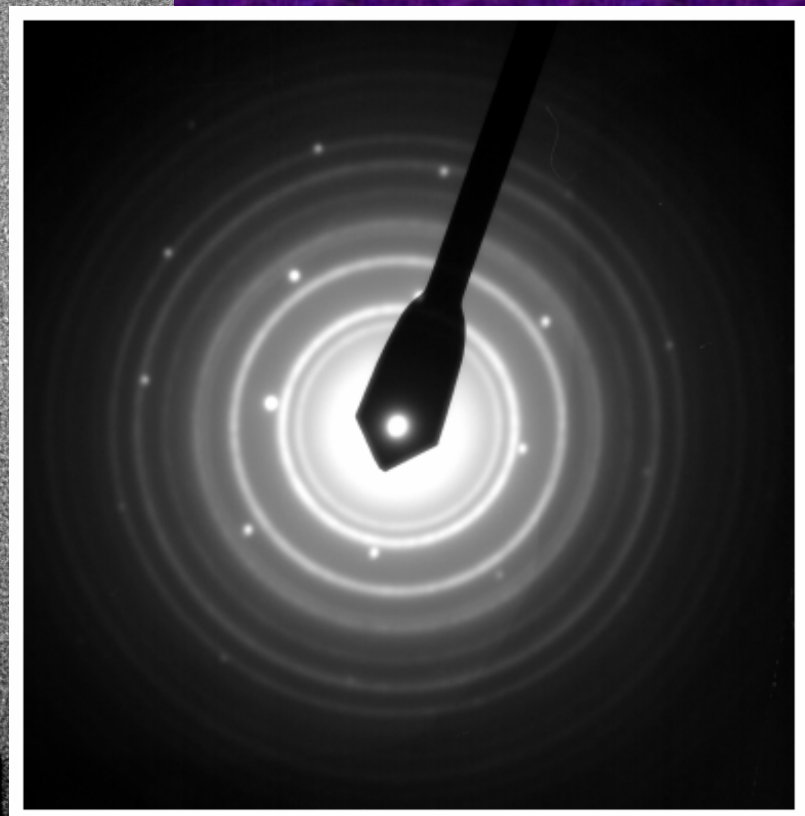

- Electron transmission micrographs and diffraction patterns revealed a polycrystalline structure, the interfaces separating densely-packed crystallites being 1-2 atomic layers thick.

T.I. Baturina, D.R. Islamov, J. Bentner, C. Strunk, M.R. Baklanov, and A. Satta, JETP Lett. 79, 337 (2004).

T.I. Baturina, C. Strunk, M.R. Baklanov, A. Satta, PRL 98, 127003 (2007).

T.I. Baturina, A.Yu. Mironov, V.M. Vinokur, M.R. Baklanov, and C. Strunk, cond-mat/0705.1602

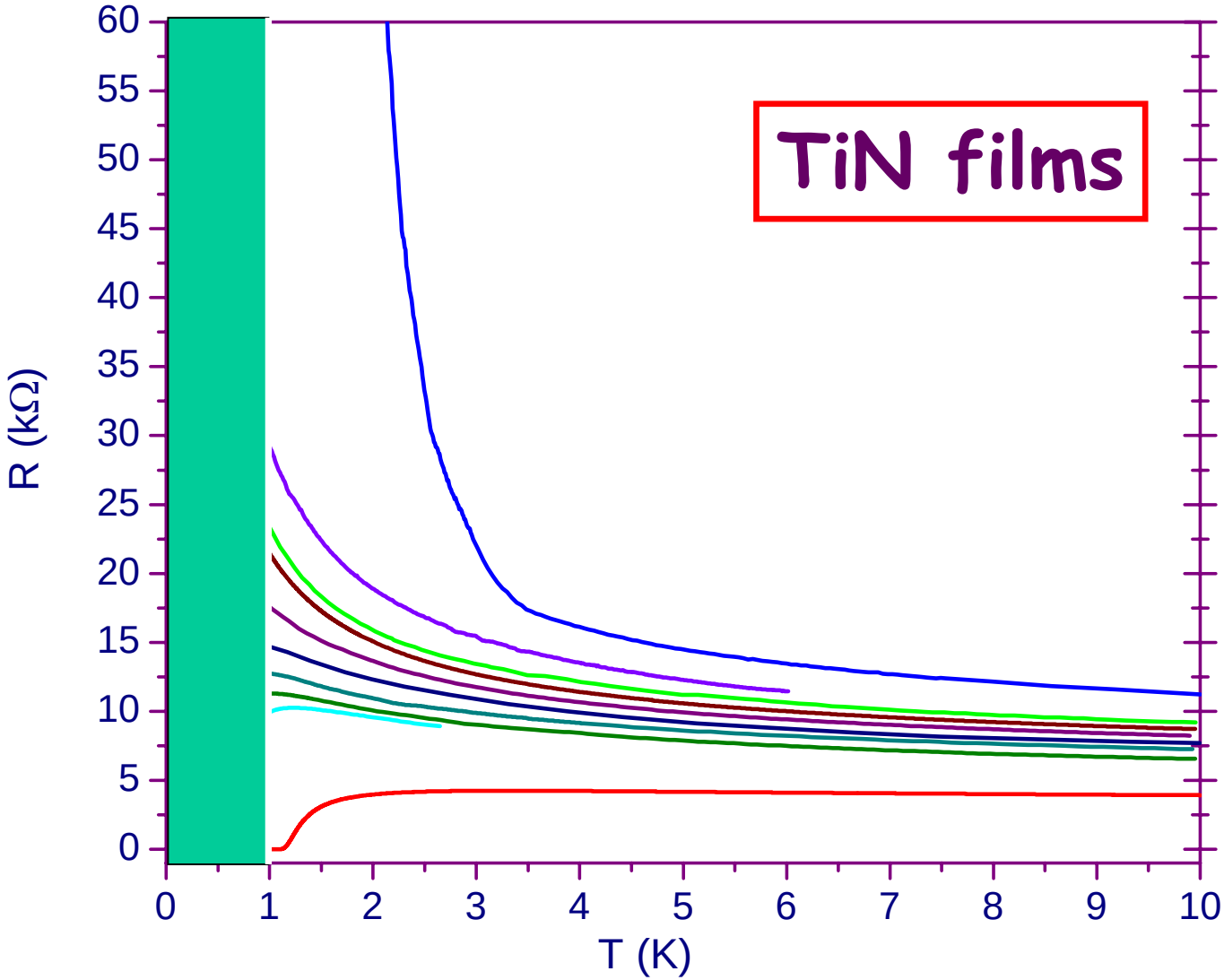

T.I. Baturina, D.R. Islamov, J. Bentner, C. Strunk, M.R. Baklanov, and A. Satta, JETP Lett. 79, 337 (2004).

T.I. Baturina, C. Strunk, M.R. Baklanov, A. Satta, PRL 98, 127003 (2007).

T.I. Baturina, A.Yu. Mironov, V.M. Vinokur, M.R. Baklanov, and C. Strunk, cond-mat/0705.1602

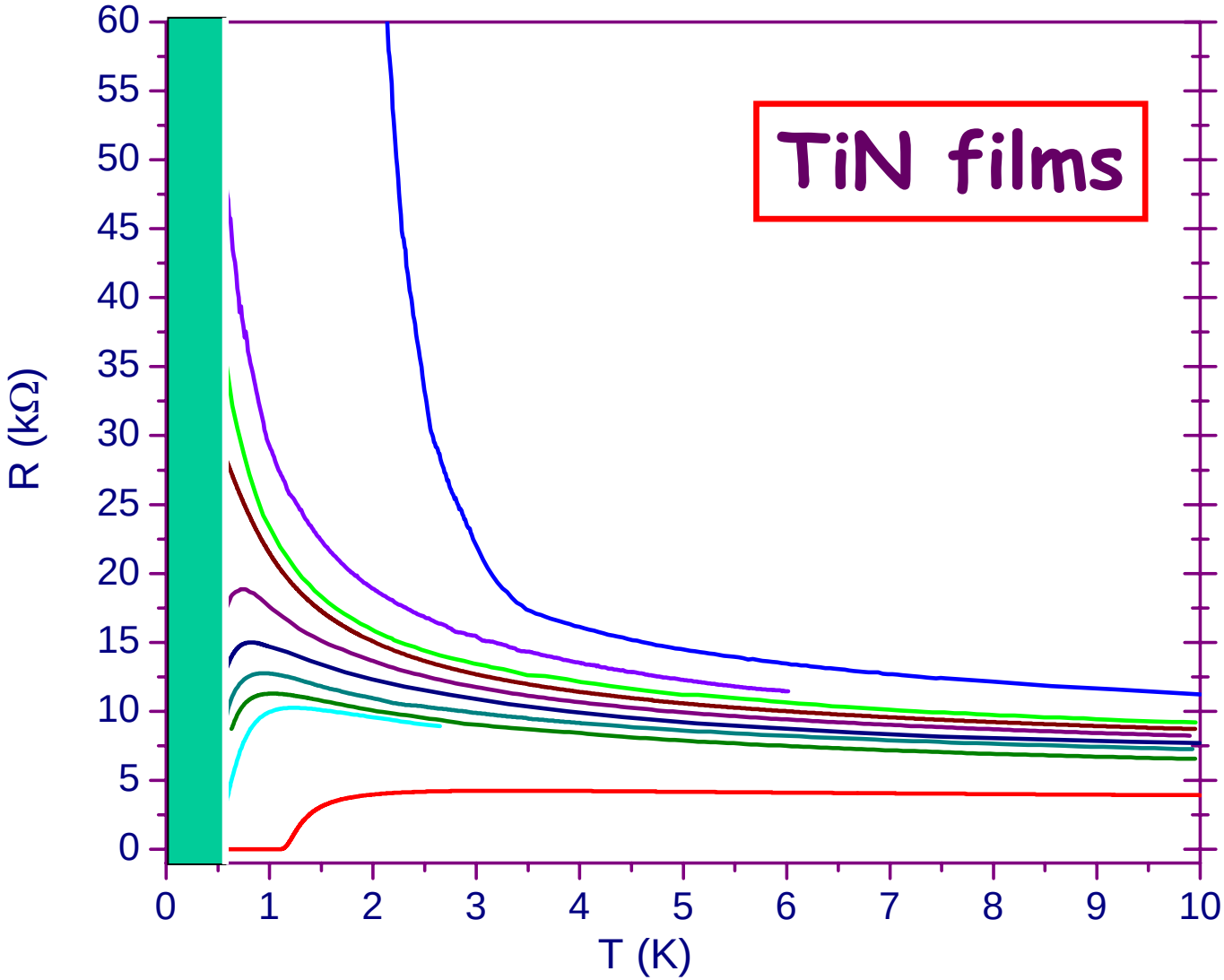

T.I. Baturina, D.R. Islamov, J. Bentner, C. Strunk, M.R. Baklanov, and A. Satta, JETP Lett. 79, 337 (2004).

T.I. Baturina, C. Strunk, M.R. Baklanov, A. Satta, PRL 98, 127003 (2007).

T.I. Baturina, A.Yu. Mironov, V.M. Vinokur, M.R. Baklanov, and C. Strunk, cond-mat/0705.1602

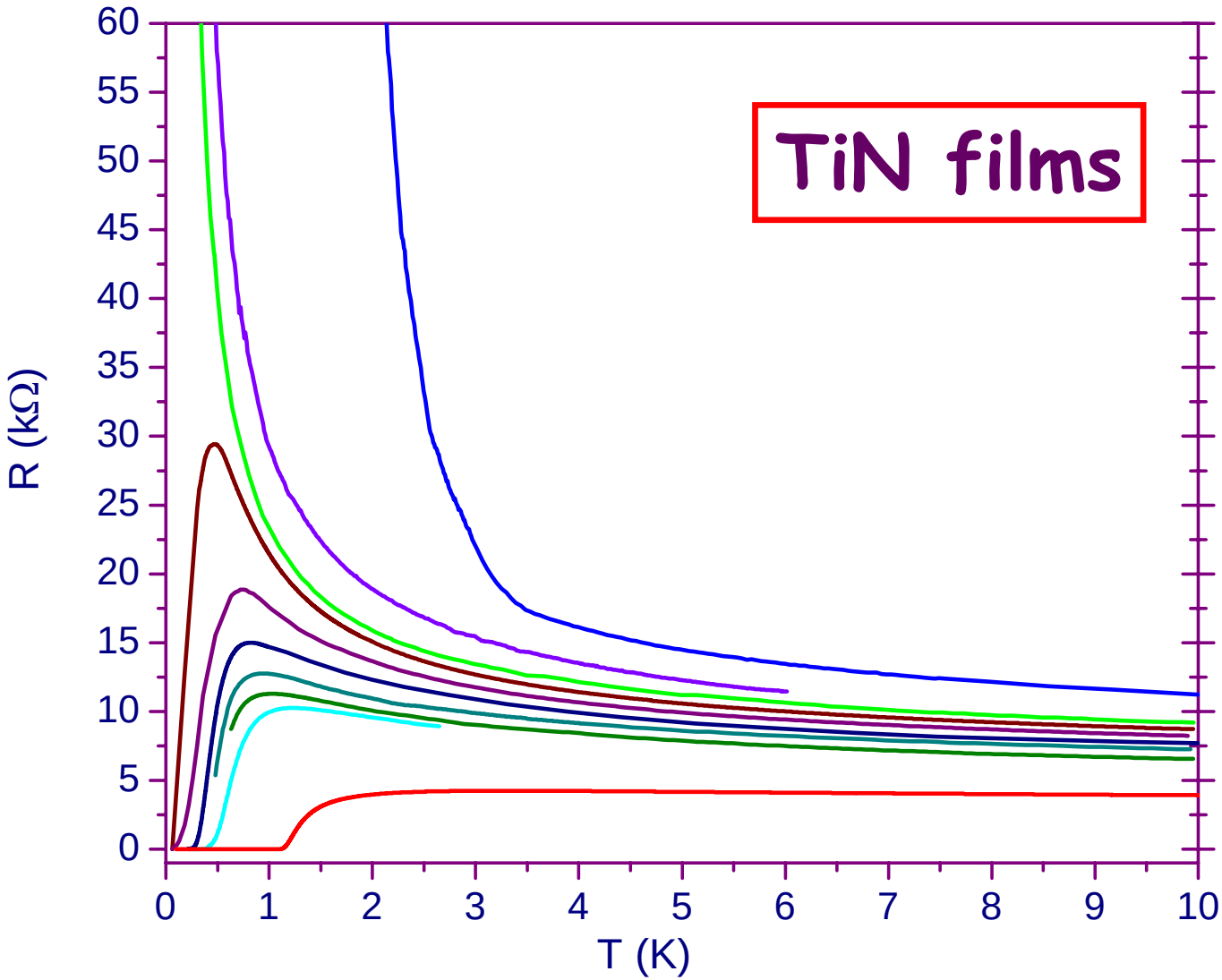

T.I. Baturina, D.R. Islamov, J. Bentner, C. Strunk, M.R. Baklanov, and A. Satta, JETP Lett. 79, 337 (2004).

T.I. Baturina, C. Strunk, M.R. Baklanov, A. Satta, PRL 98, 127003 (2007).

T.I. Baturina, A.Yu. Mironov, V.M. Vinokur, M.R. Baklanov, and C. Strunk, cond-mat/0705.1602

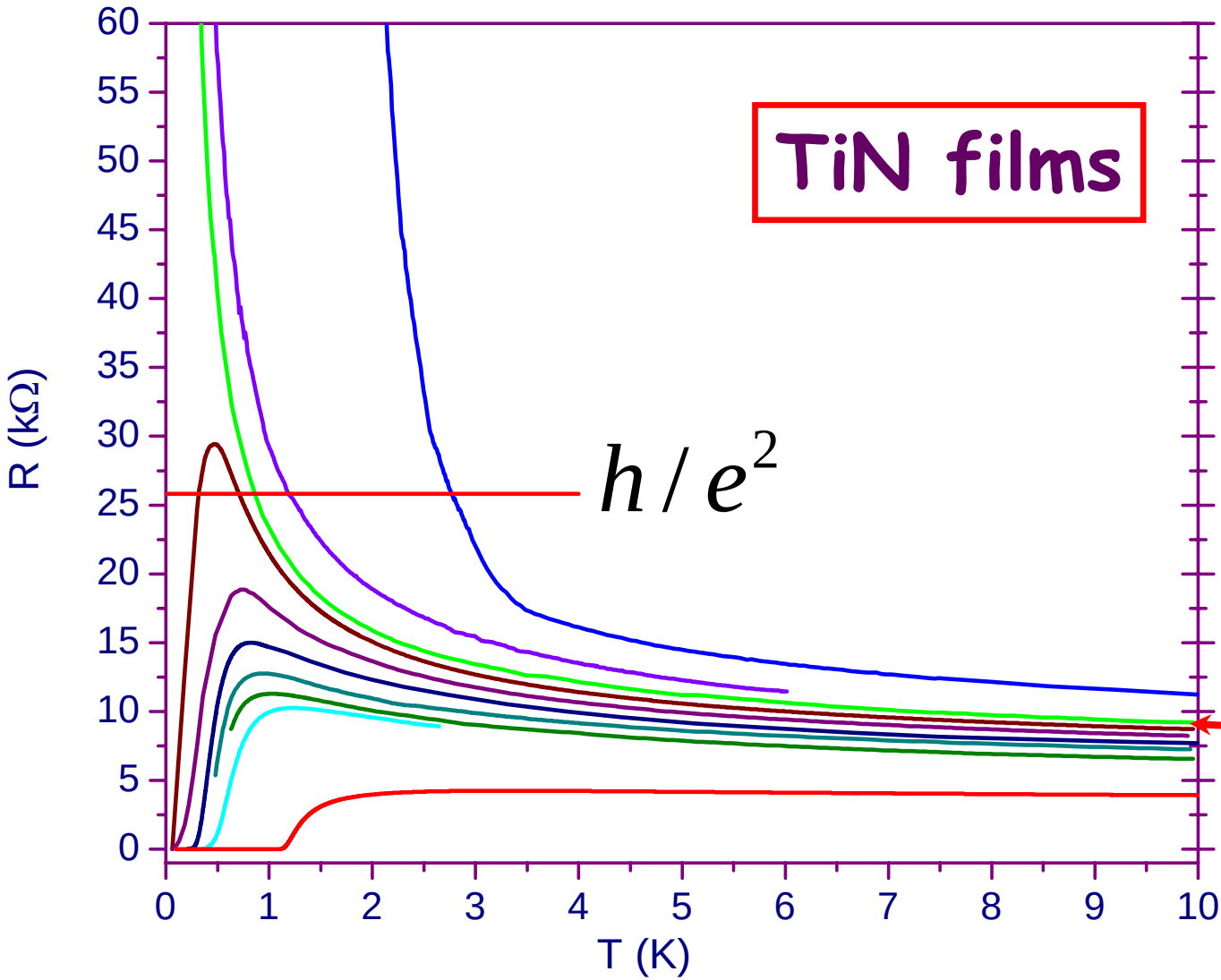

TiN films

$R_c \approx 10\ k\Omega$

SMIT or SIT

The search for a disorder-driven superconductor-insulator transition has included many materials, e.g.,

Bi, MoSi, Ta, InO_x, Be, TiN.

The immediate onset of exponential temperature dependence of the resistance, which conclusively evidences

the direct transition into an insulator,

was found so far only in **InO_x**, **Be**, and **TiN** films.

For **Bi**, **MoSi**, and **Ta**-compounds a weak logarithmic temperature dependence of the resistance was observed on the nonsuperconducting side in the vicinity of the transition.

- ✓ This possibly indicates an intermediate metallic phase
- ✓ More studies at even lower temperatures are needed to obtaine conclusive evidences on which films fall into a superconducting state and which become insulating state

SIT

Suppression of Superconductivity by Disorder

The immediate onset of exponential temperature dependence of the resistance, which conclusively evidences **the direct transition into an insulator,**

was found so far only in **InO_x** , **Be**, and **TiN** films.

Insulating side of the transition
InO_x, **Be**, and **TiN** films

TiN films

T.I. Baturina, A.Yu. Mironov, V.M. Vinokur, M.R. Baklanov, and C. Strunk, cond-mat/0705.1602

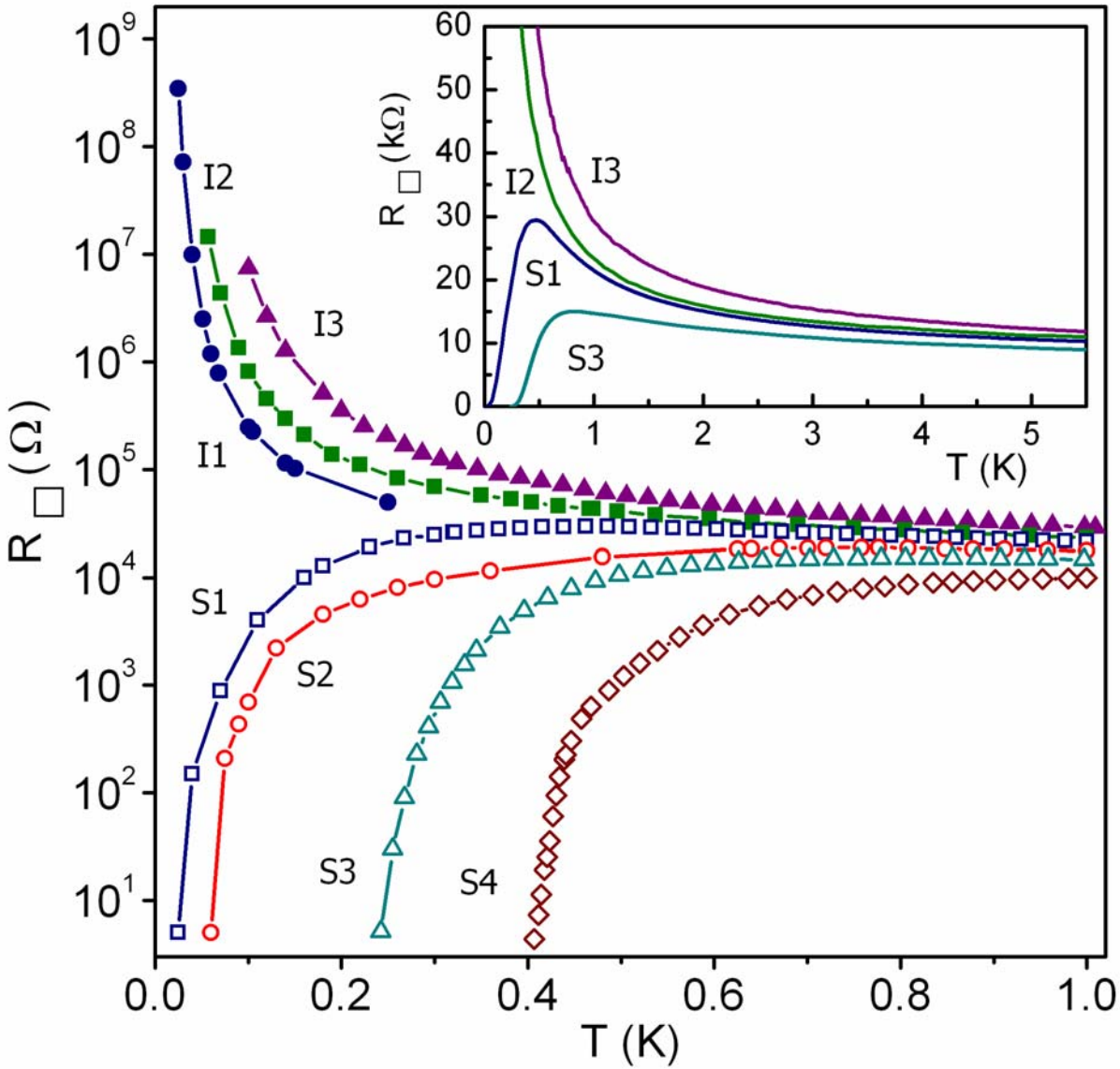

TiN films

T.I. Baturina, A.Yu. Mironov, V.M. Vinokur, M.R. Baklanov, and C. Strunk, cond-mat/0705.1602

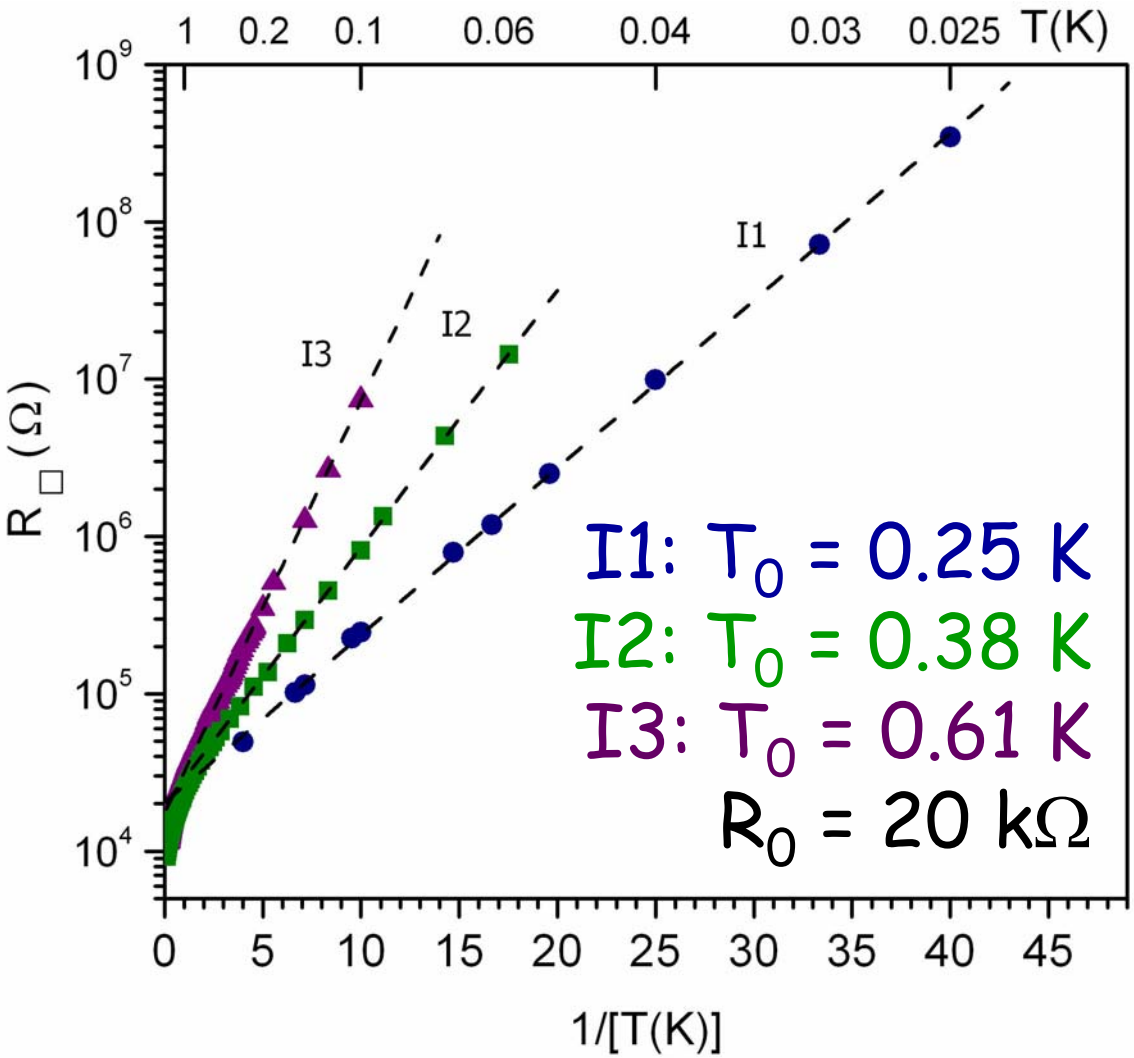

I1: T_0 = 0.25 K

I2: T_0 = 0.38 K

I3: T_0 = 0.61 K

R_0 = 20 kΩ

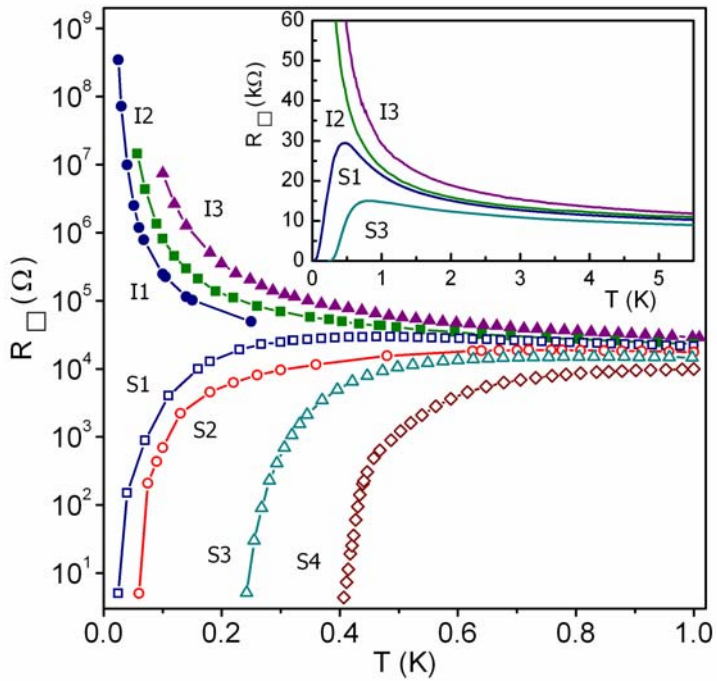

$R = R_0 \exp(T_0/T)$

At low temperatures we observe an Arrhenius behavior of the resistance

TiN films

T.I. Baturina, A.Yu. Mironov, V.M. Vinokur, M.R. Baklanov, and C. Strunk, cond-mat/0705.1602

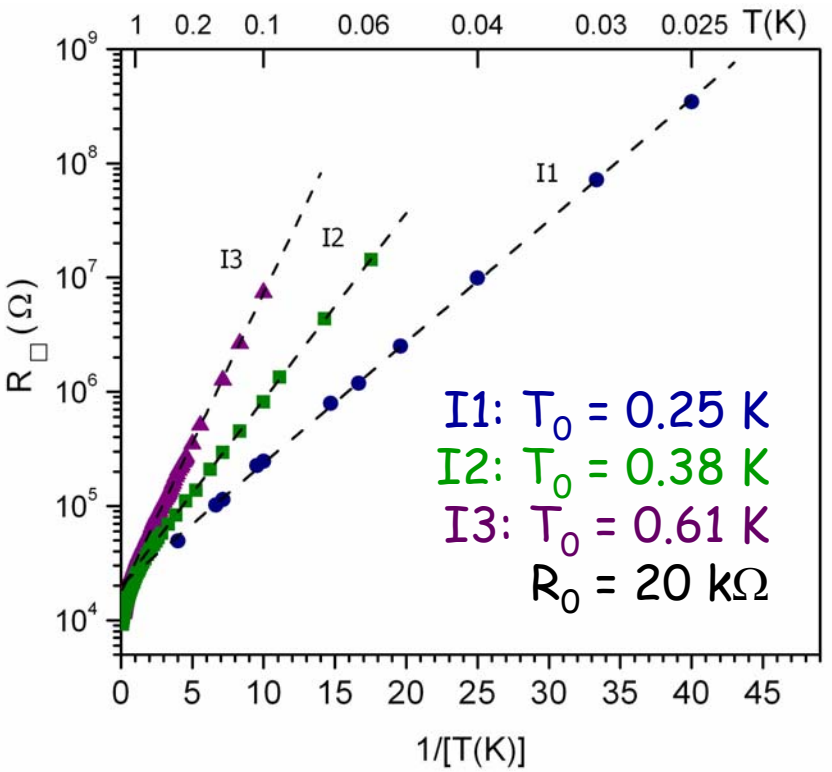

$$R = R_0 \exp(T_0/T)$$

At low temperatures we observe an Arrhenius behavior of the resistance

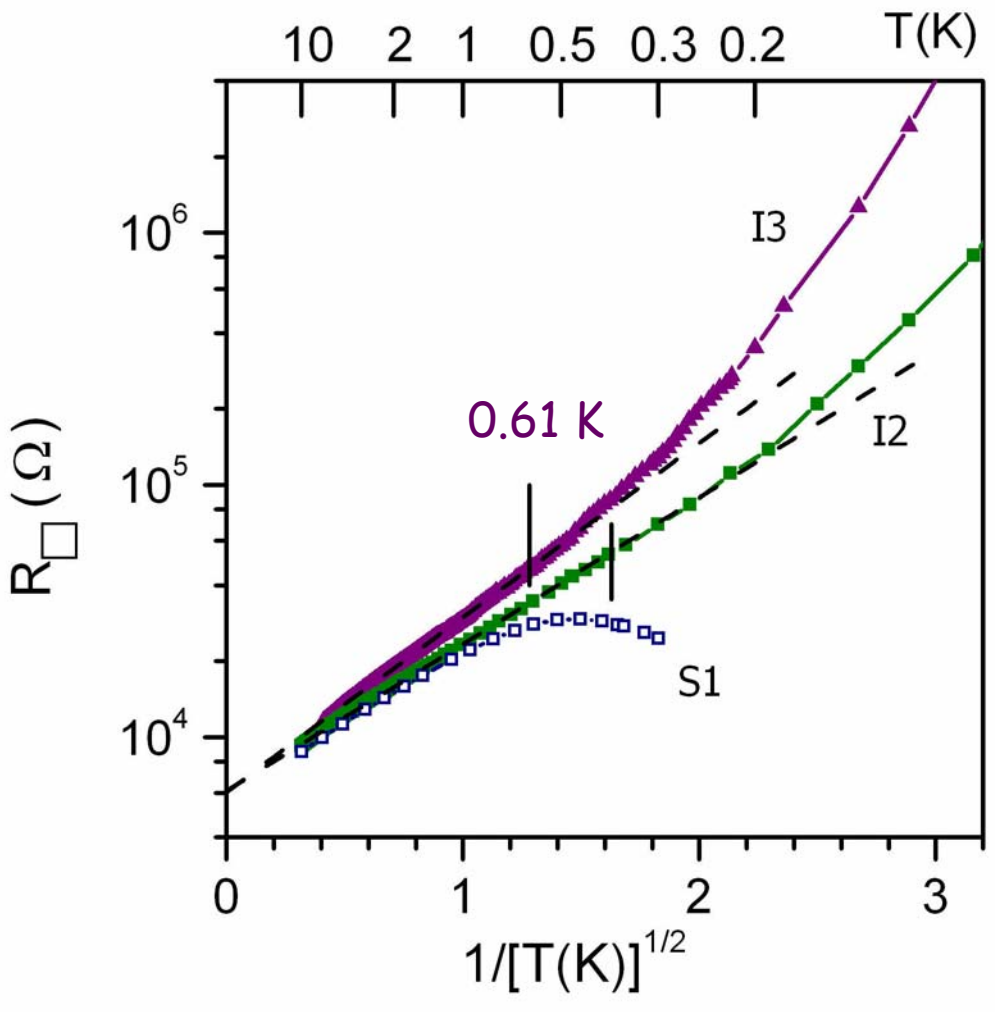

$$R = R_1 \exp(T_1/T)^{1/2}$$

Be films

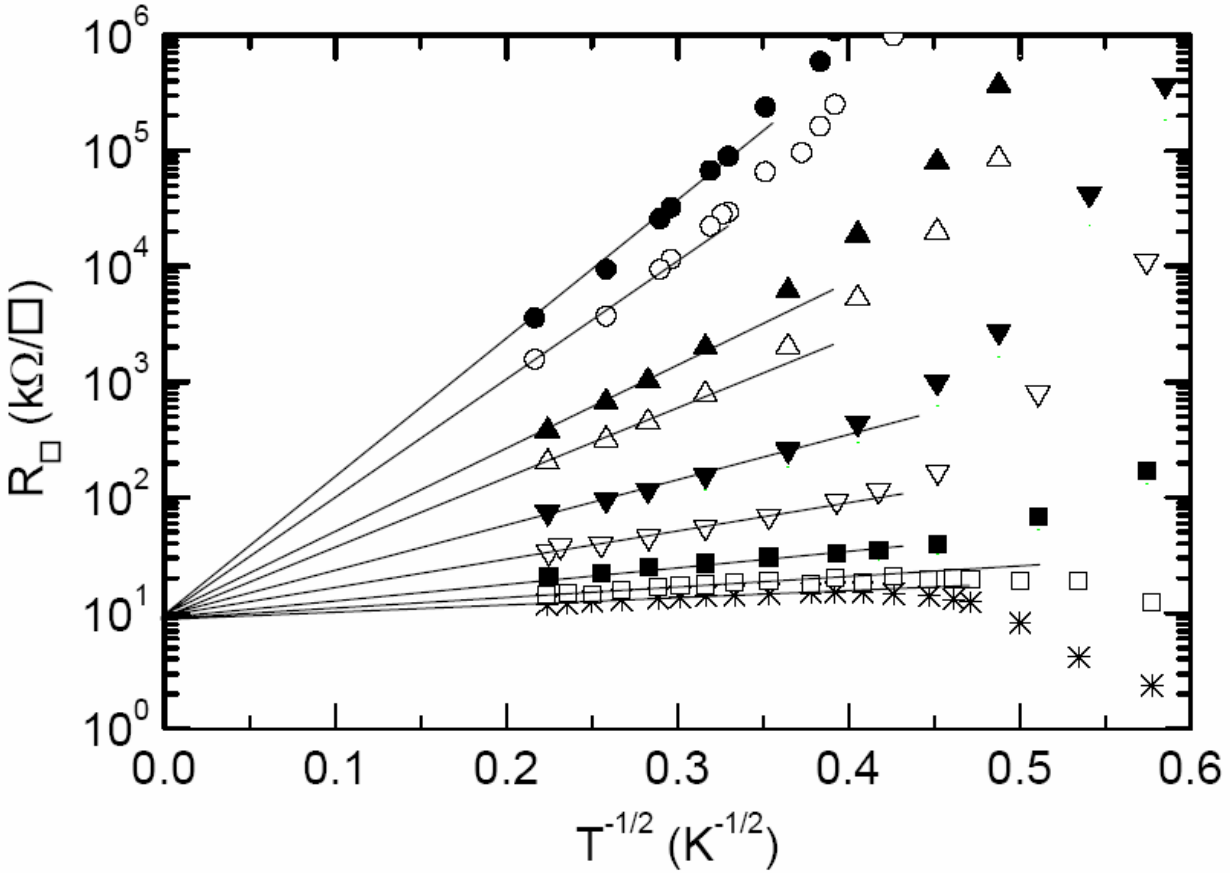

W. Wu and E. Bielejec, cond-mat/051121.

Fig. 1 Selected curves of $R_\square$ versus $1/T^{1/2}$ for one Be film section following deposition steps to increase film thickness (from top to bottom). The thickness for these films changed from 4.6 Å to about 10 Å. The straight lines are draw as a guide for eye, showing that in the high-T regime all the curves follow straight lines that converge to about 10 kΩ/□ in the $T \rightarrow \infty$ limit. The films for bottom curve is superconducting at low temperatures.

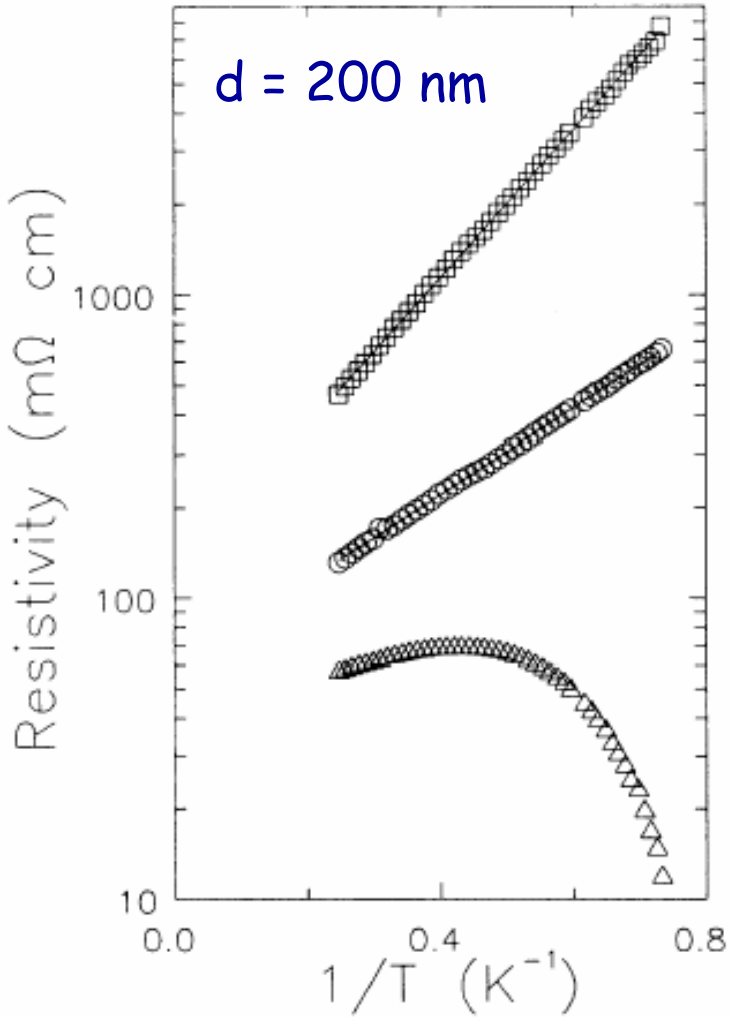

FIG. 2. Resistivity vs temperature of a typical batch of indium-oxide samples measured between 1.3 and 4.11 K. The upper curve is for the as-deposited film. The lower curves depict the $R(T)$ of the same sample after thermal annealing. The solid lines for the top two curves are fits to an Arrhenius behavior from which the various T_0 values were extracted. $k_F l$ values of these samples are 0.177 (□), 0.21 (○), and 0.272 (△). The sample thickness is 2000 Å and $n = 4 \times 10^{21}$.

InO_x films

D. Shahar and Z. Ovadyahu, PRB 46, 10917 (1992).

InO_x film

D. Kowal and Z. Ovadyahu
Solid State Comm. 90,
783 (1994).

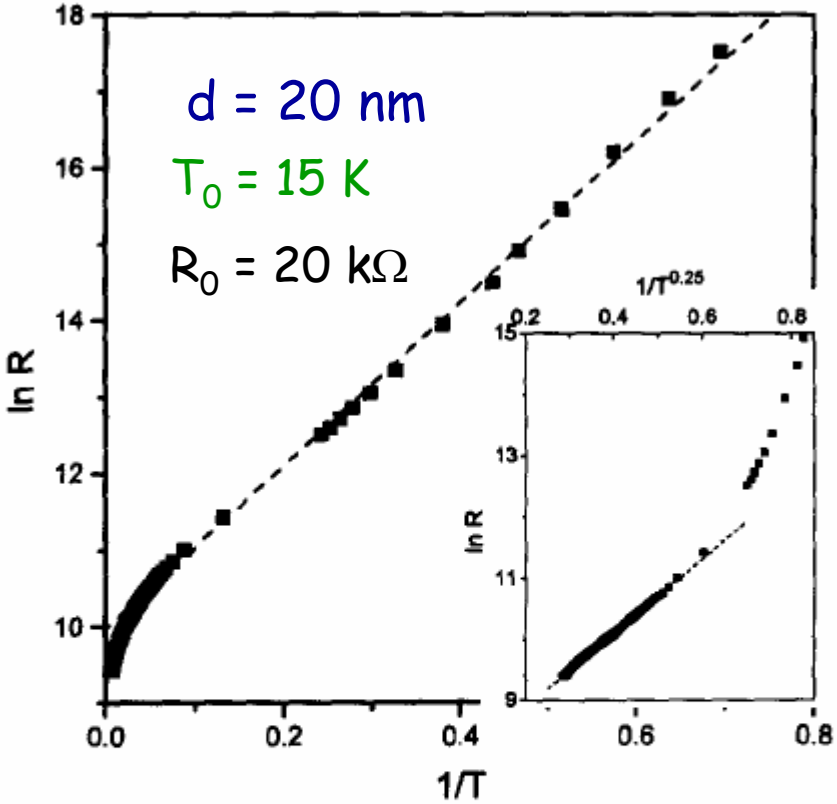

Fig. 1. The temperature dependence of the resistance for a 200Å thick sample in the range 1.4K-200K. Below 4.1K simple activation is observed with T_0=15K. Inset: The same data plotted against $T^{1/4}$ exhibits 3D VRH above 10K. The localization length determined from the slope and the known density of electrons is 12Å.

TiN film

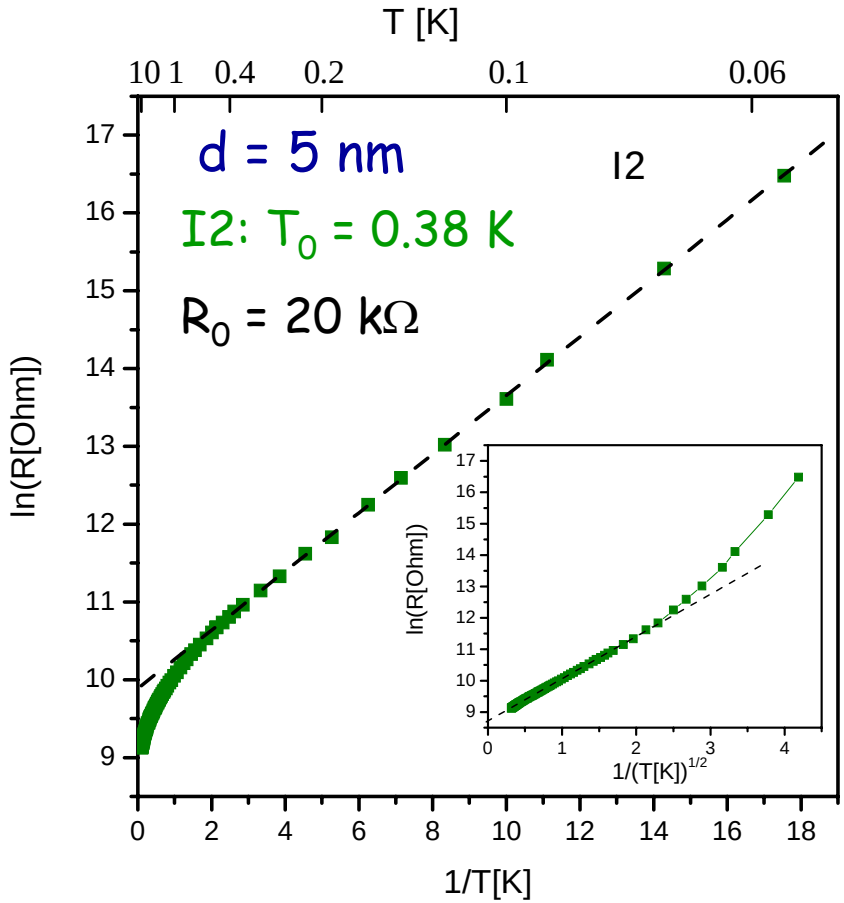

Insulating side of the transition
InO_x, Be, and TiN films

- at low temperatures
- activation law

$$R = R_0 \exp(T_0/T)$$

- at temperatures higher than T_0

InO_x films

- 3D Mott's VRH

$$R = R_1 \exp(T_1/T)^{1/4}$$

Be and TiN films

- the ES hopping

$$R = R_1 \exp(T_1/T)^{1/2}$$

T.I. Baturina, D.R. Islamov, J. Bentner, C. Strunk, M.R. Baklanov, and A. Satta, JETP Lett. 79, 337 (2004).

T.I. Baturina, C. Strunk, M.R. Baklanov, A. Satta, PRL 98, 127003 (2007).

T.I. Baturina, A.Yu. Mironov, V.M. Vinokur, M.R. Baklanov, and C. Strunk, cond-mat/0705.1602

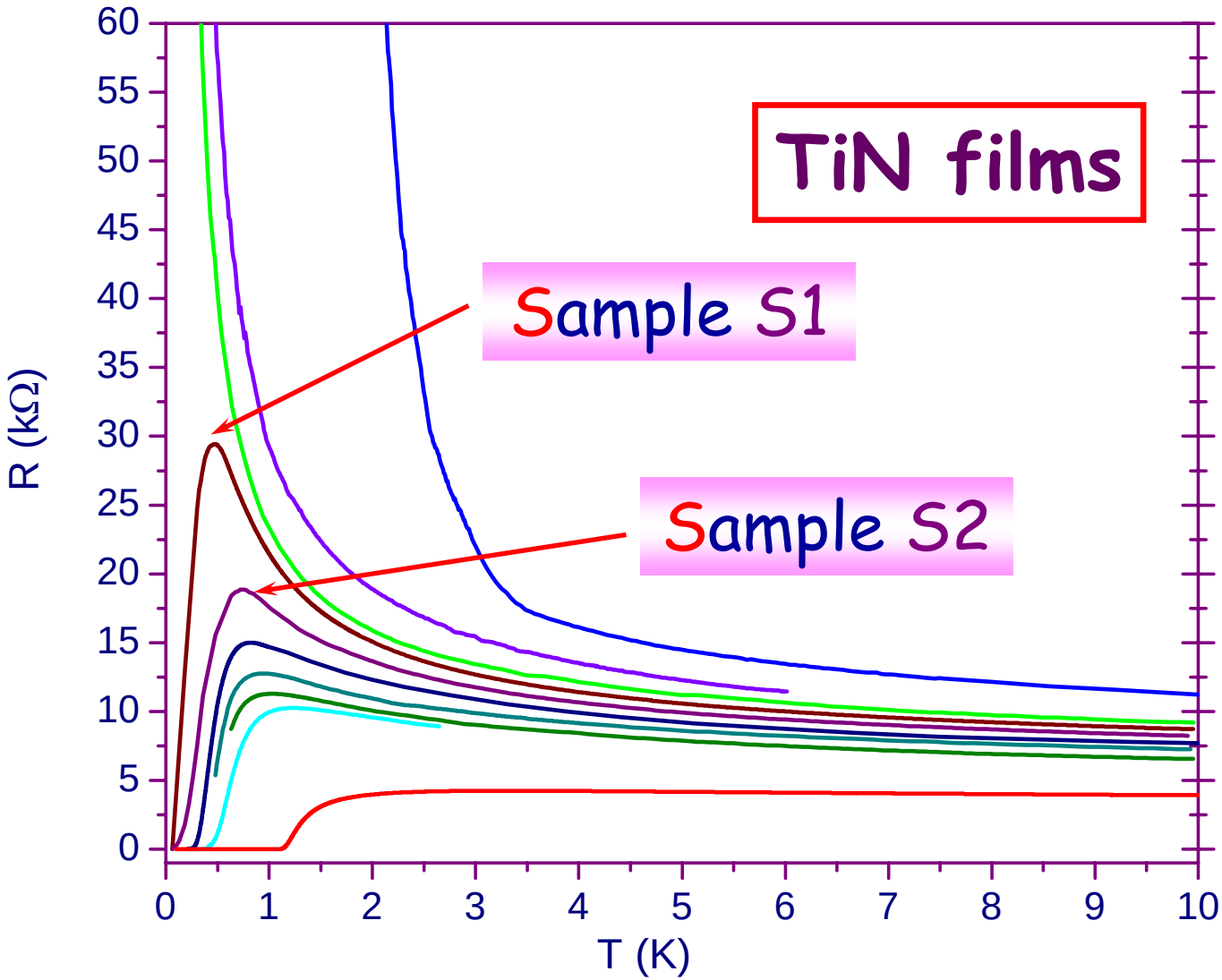

Experiment

T. Baturina, C. Strunk, M.R. Baklanov, A. Satta
PRL 98, 127003 (2007)

Magnetic-field-tuned superconductor – insulator quantum phase transition

Sample S1

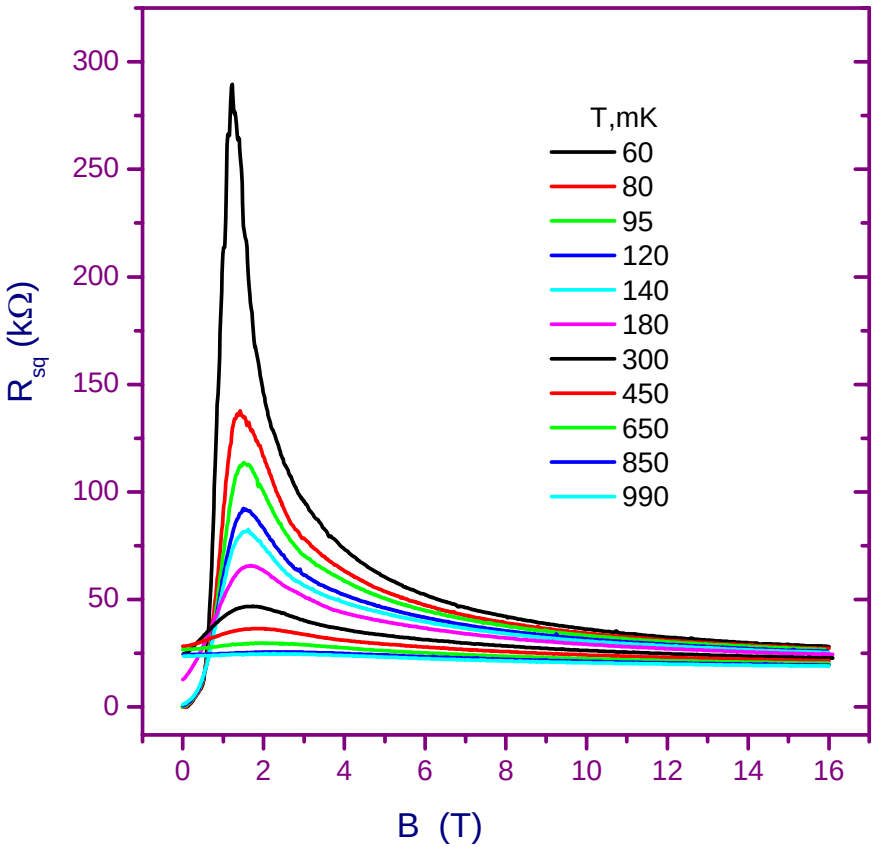

Sample S2

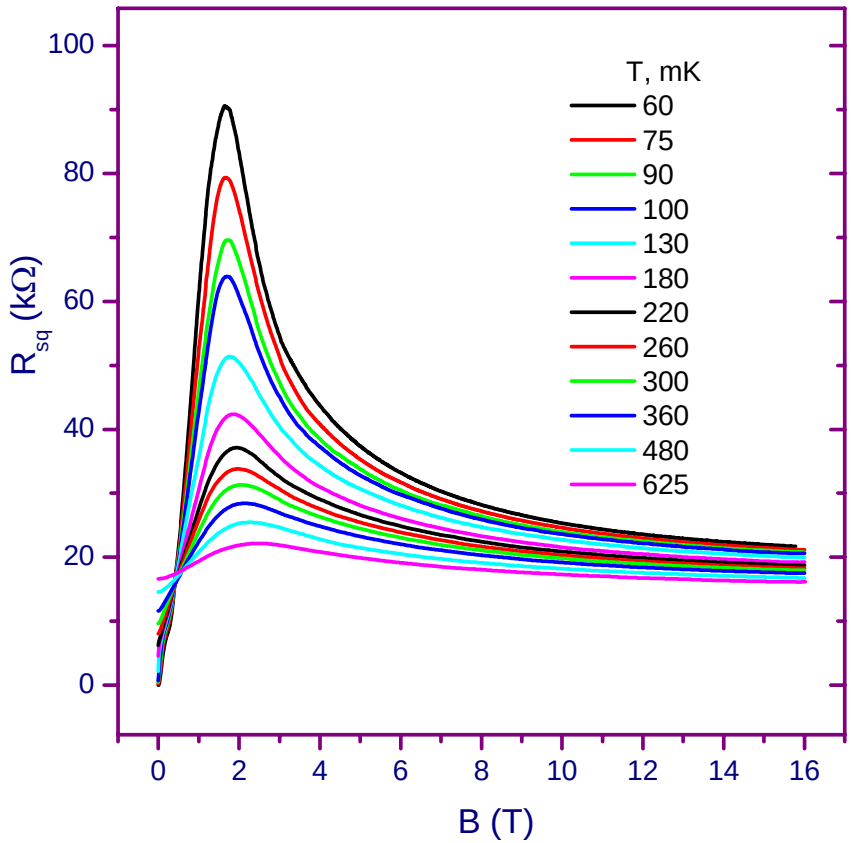

Experiment

Magnetic-field-tuned superconductor – insulator quantum phase transition

Sample S1

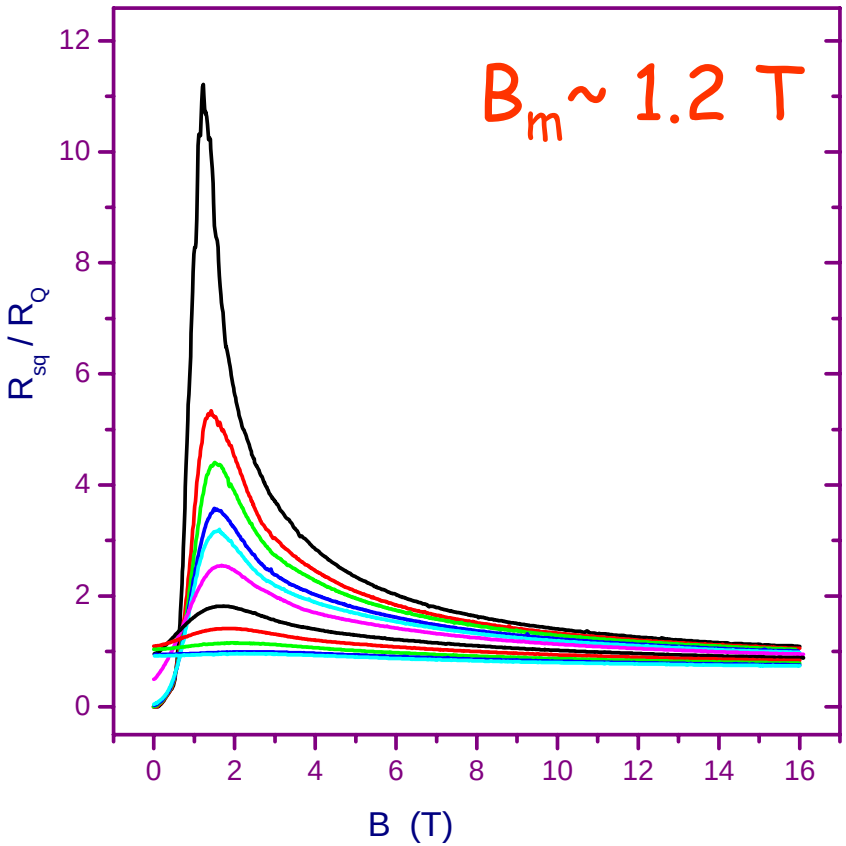

Sample S2

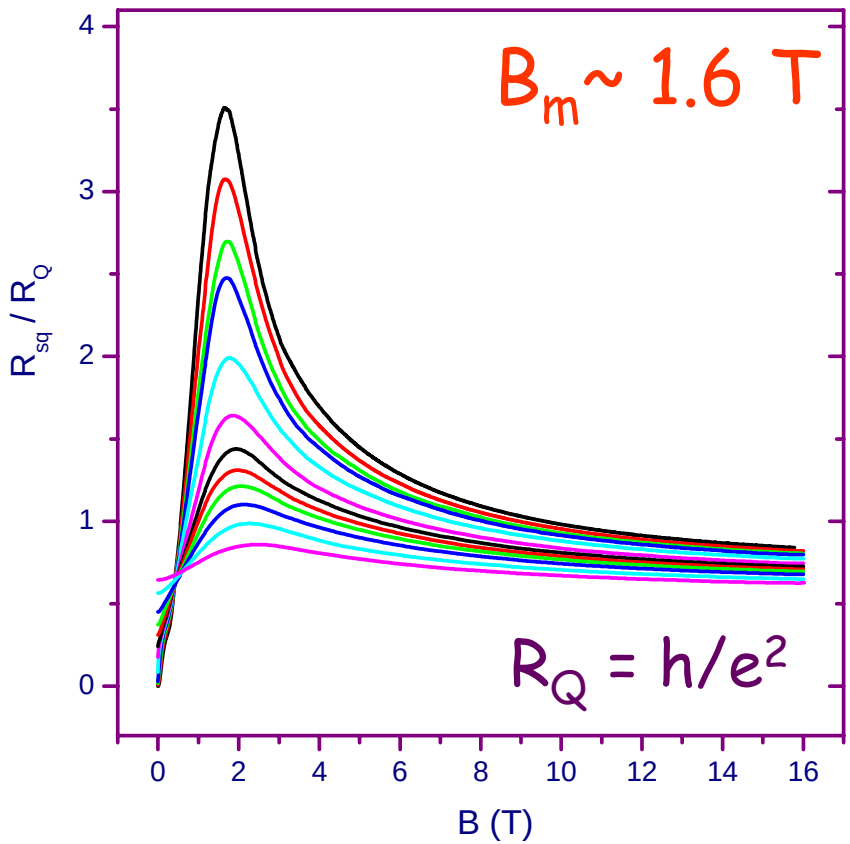

The saturation occurs at a resistance R_{sat}

near the quantum resistance h/e^2 !!!

Sample S1

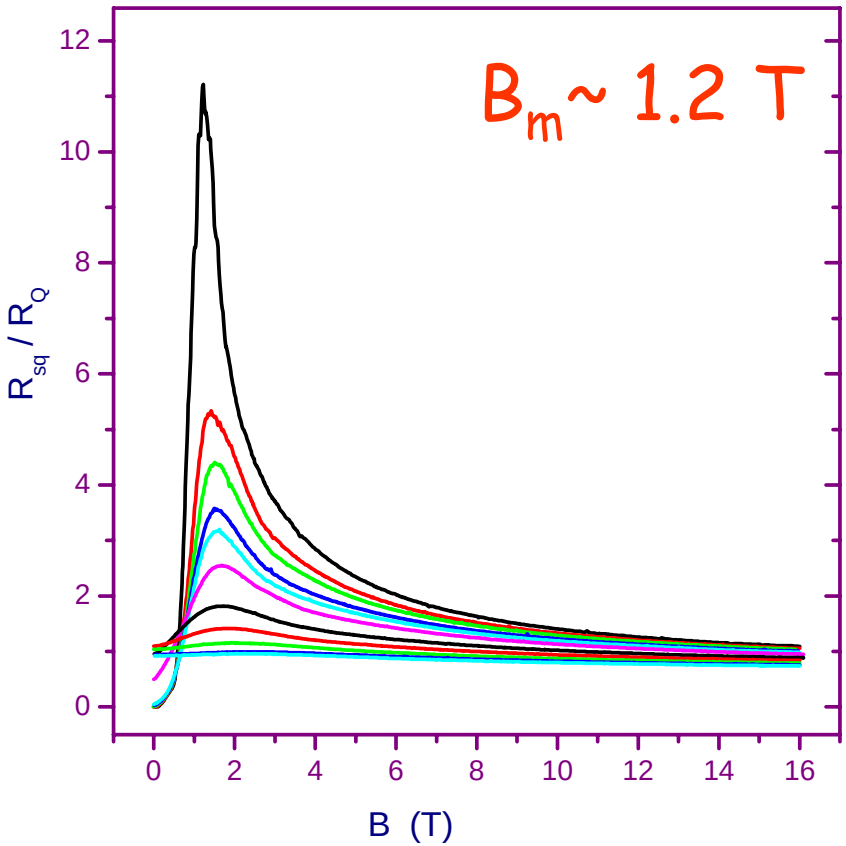

Sample S2

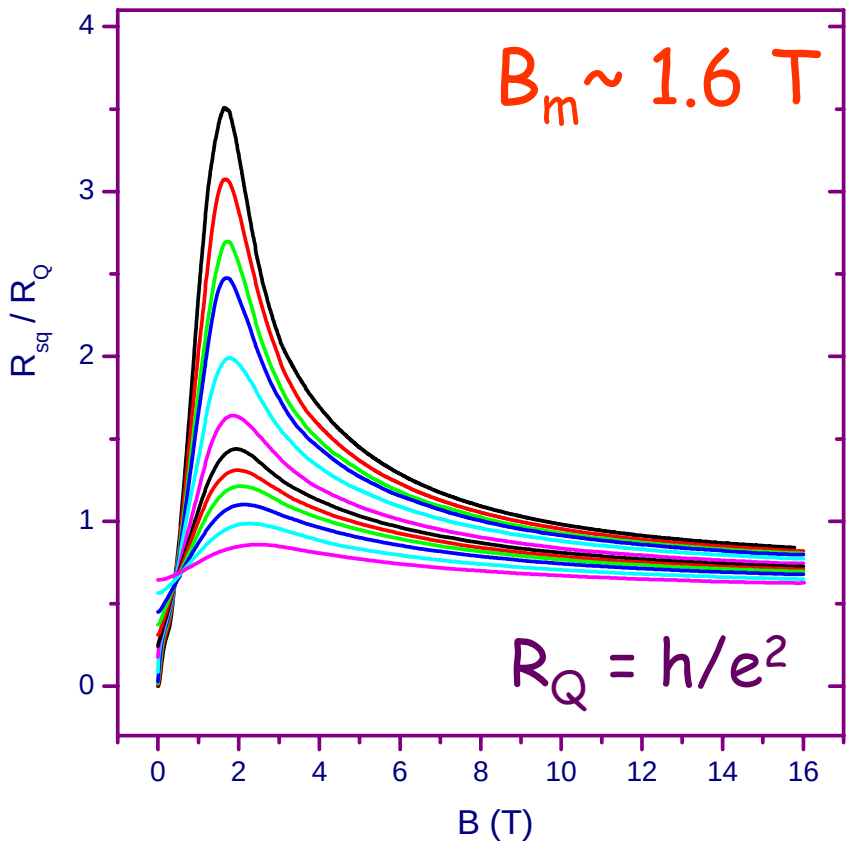

by varying the value of R_{sat} for each curve , we can linearize

$\ln(1/R_{sat} - 1/R_{sq}(B))$ vs. B

over a large range of B
with T-independent slope !!!

Sample A

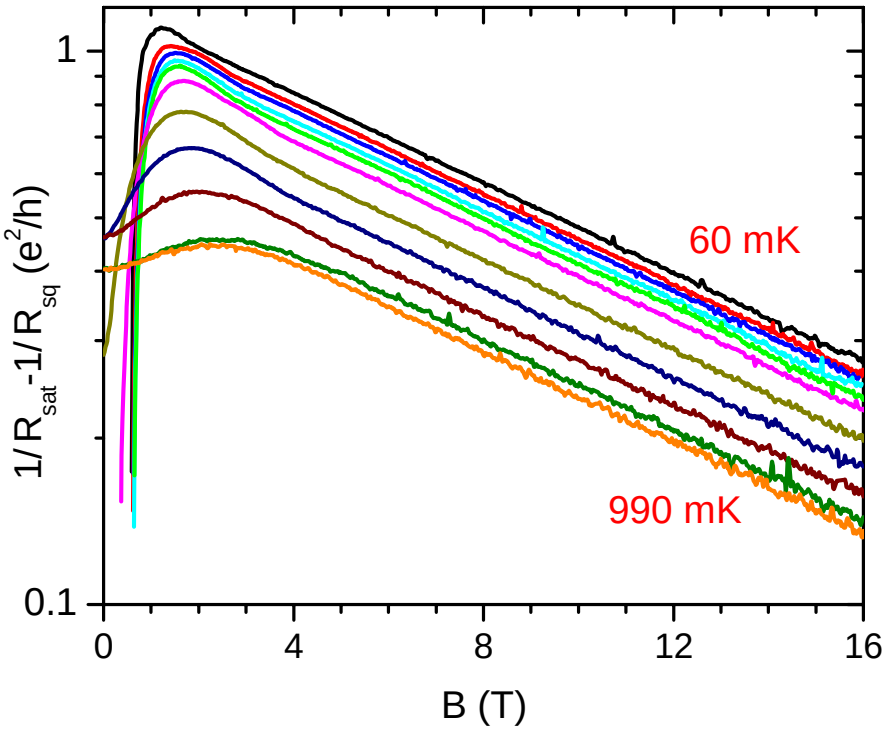

Sample B

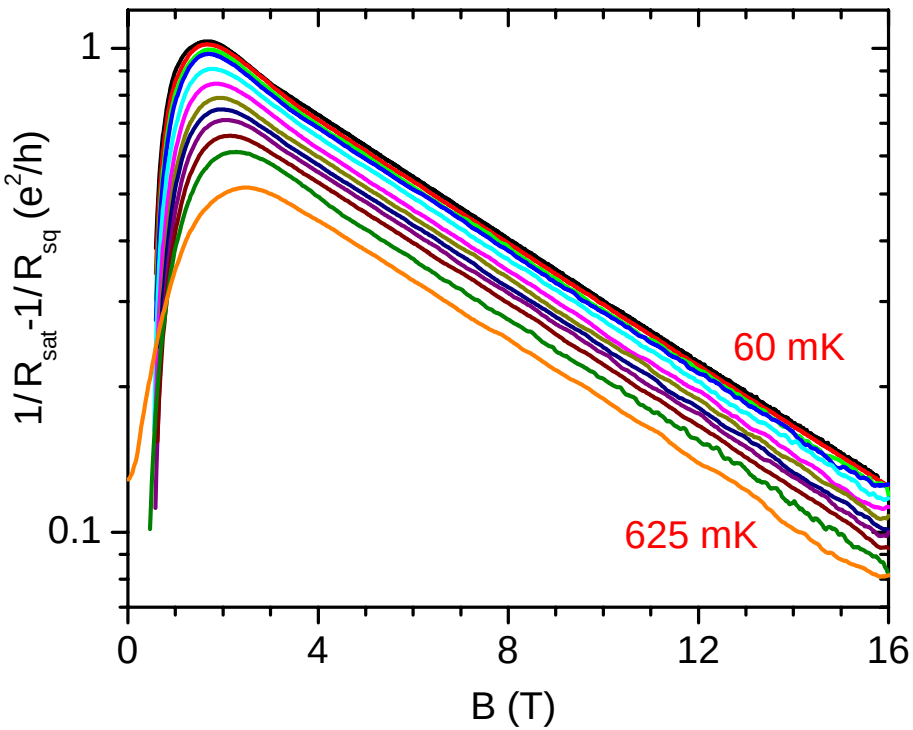

by varying the value of R_{sat} for each curve , we can linearize

$\ln(1/R_{sat} - 1/R_{sq}(B))$ vs. B

over a large range of B
with T-independent slope !!!

$$G_{sq}(T,B)[=1/R_{sq}(T,B)] = 1/R_{sat}(T) - \beta(T)\exp(-B/B^*)$$

Sample A

$B^* = 10.7$ T

Sample B

$B^* = 6.8$ T

$$G_{sq}(T,B)[=1/R_{sq}(T,B)] = 1/R_{sat}(T) - \beta(T)\exp(-B/B^*)$$

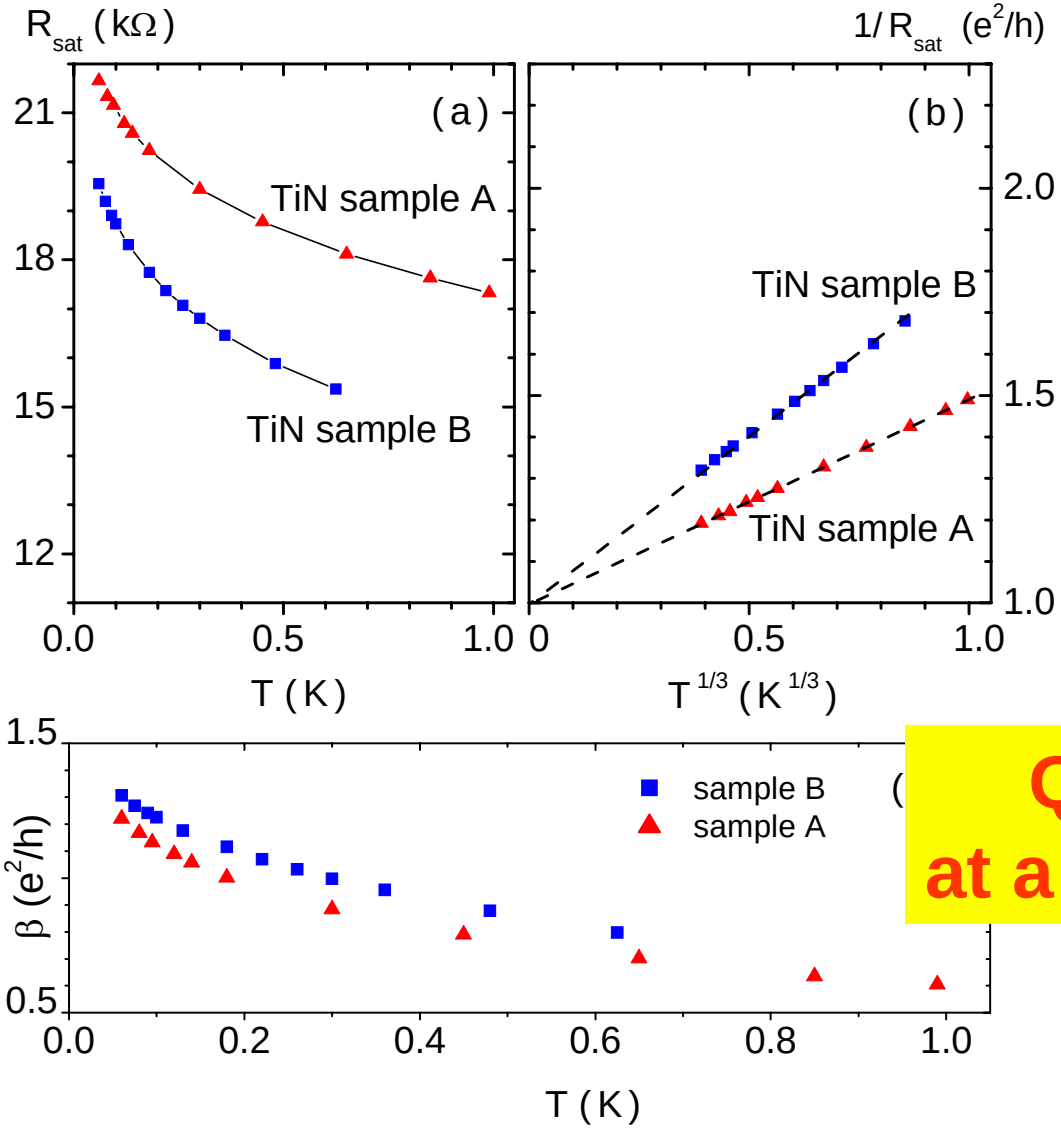

$$R_{sat}(T \rightarrow 0) \rightarrow h/e^2$$

Quantum metallicity at a high-field side of SIT

Field-induced superconductor – insulator transition

V. F. Gantmakher, M. V. Golubkov, V. T. Dolgopolov, A. A. Shashkin, G. E. Tsydynzhapov, JETP Lett. **71**, 160 (2000); **71**, 473 (2000)

a-InO_x

Fan-shaped curves

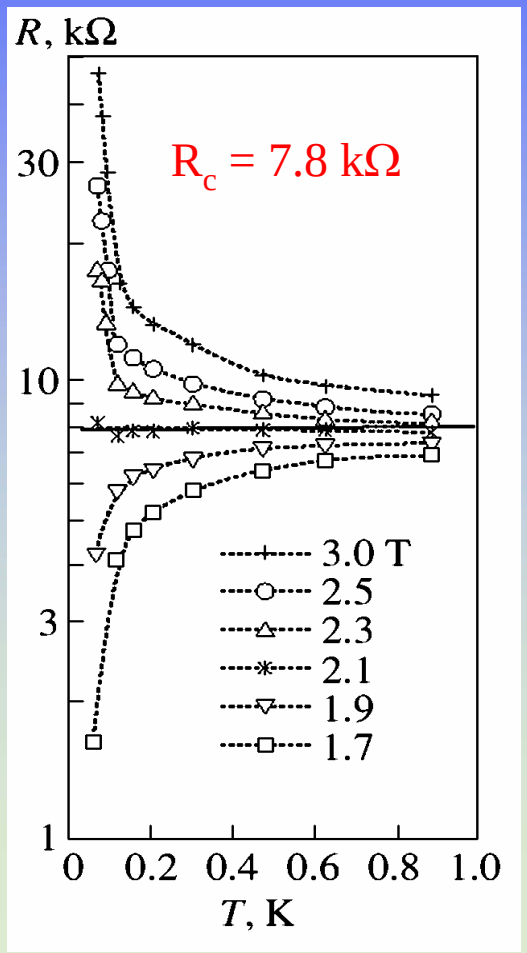

Scaling

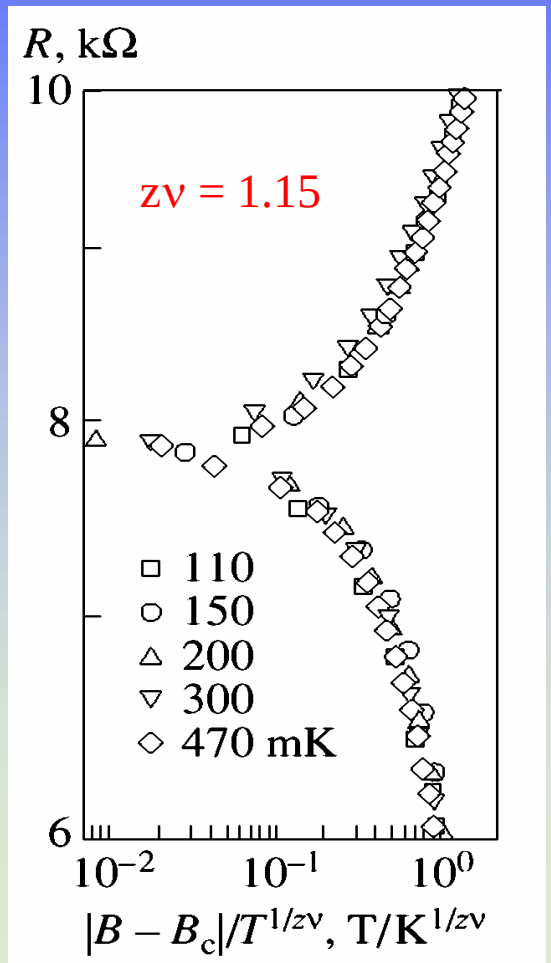

Negative magnetoresistance

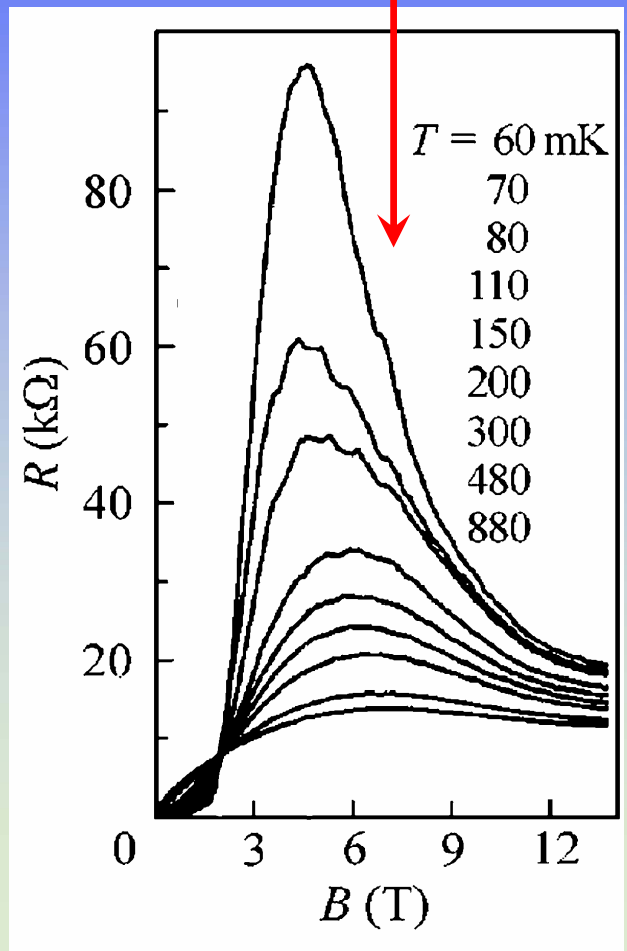

V. F. Gantmakher, M. V. Golubkov, V. T. Dolgopolov, A. A. Shashkin, G. E. Tsydynzhapov, JETP Lett. **64**, 363 (1998).

InO_x film

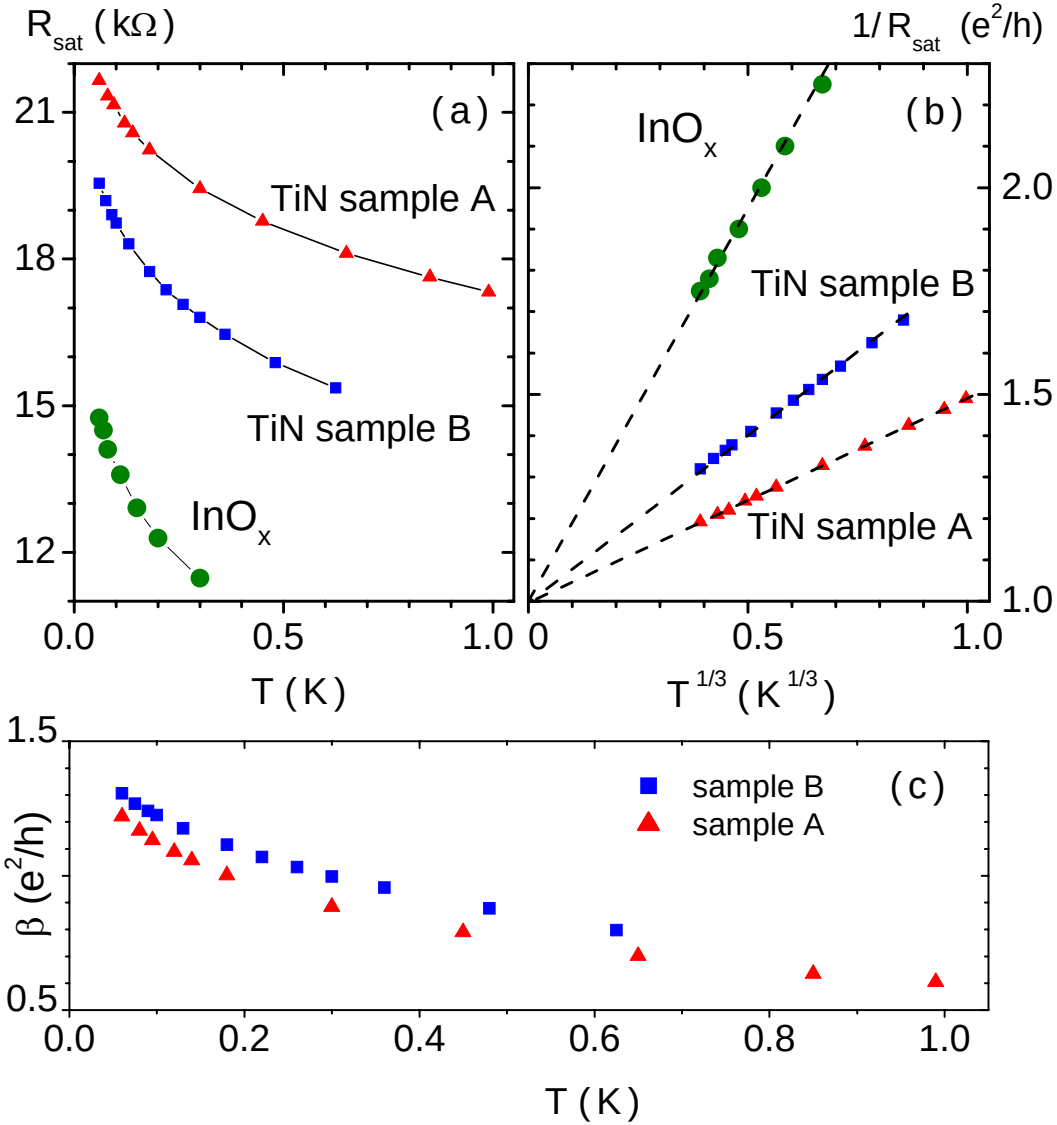

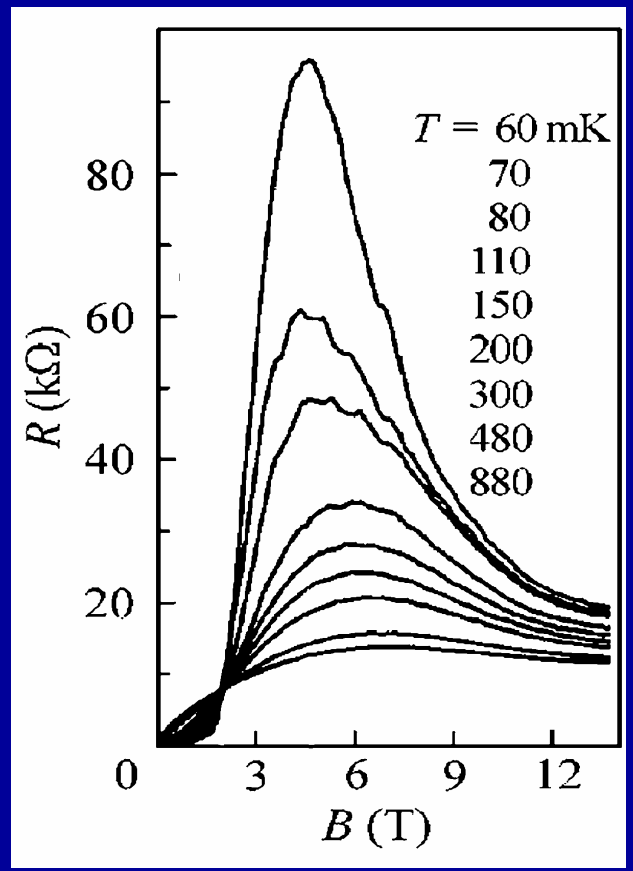

Quantum metallicity in a two-dimensional insulator

Nature 409, 161 (2001)

V. Yu. Butko*† & P. W. Adams*

Be films

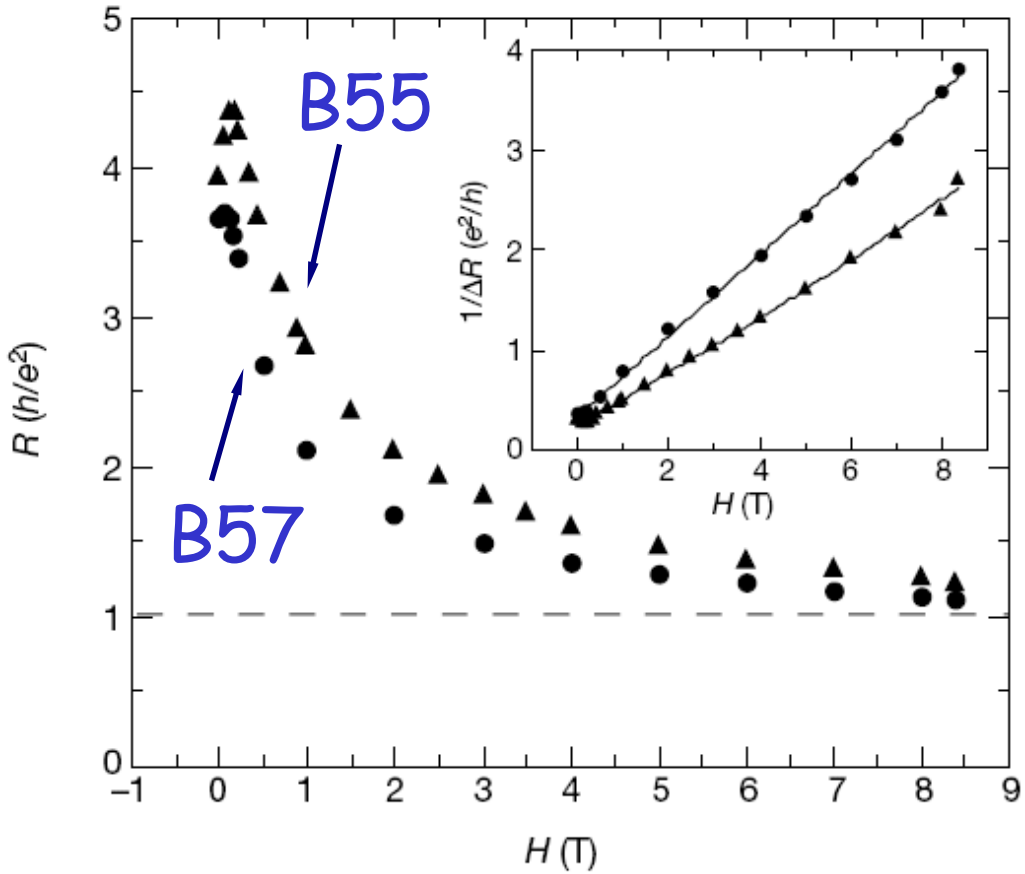

Figure 2 Low-temperature magnetoresistance. The figure shows the resistance in units of h/e^2 as a function of magnetic field H at $T = 40$ mK, for samples B57 (circles) and B55 (triangles). We note the saturation at $R \approx h/e^2$. Inset, linear behaviour after subtracting a saturation resistance of 0.85 h/e^2, $\Delta R = R - 0.85$. The solid lines are guides to the eye.

Field-induced superconductor – insulator transition

E. Bielejec and Wenhao Wu, PRL **88**, 206802 (2002)

Be films

Fan-shaped curves

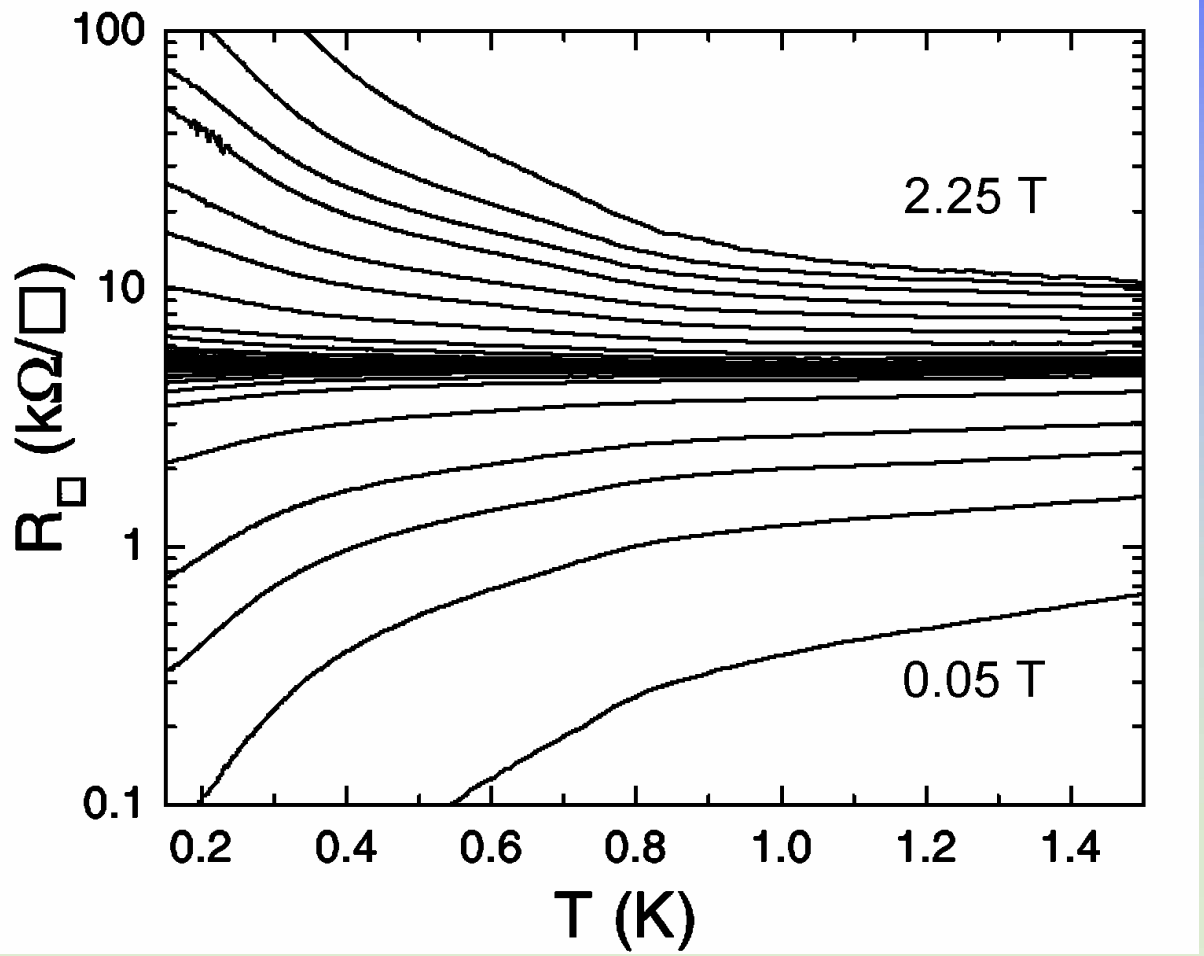

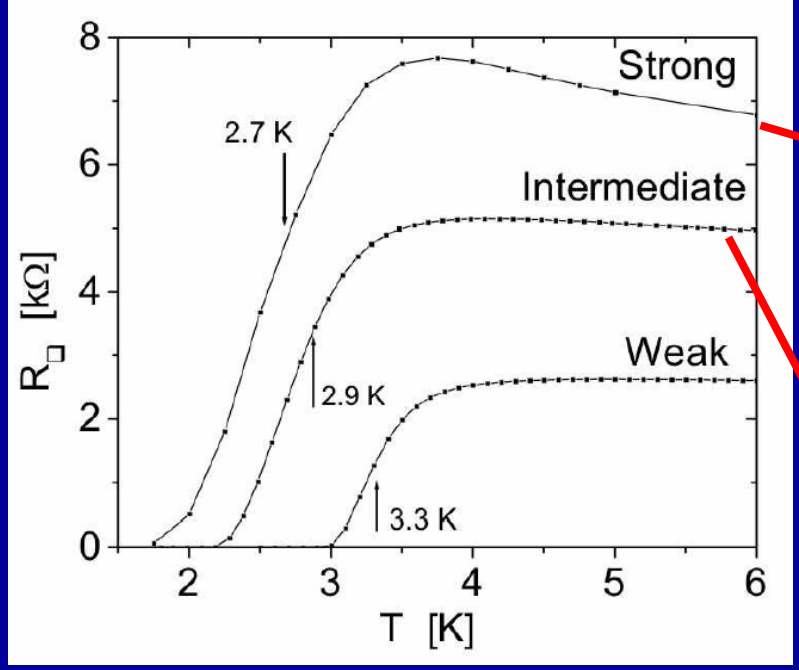

SIT

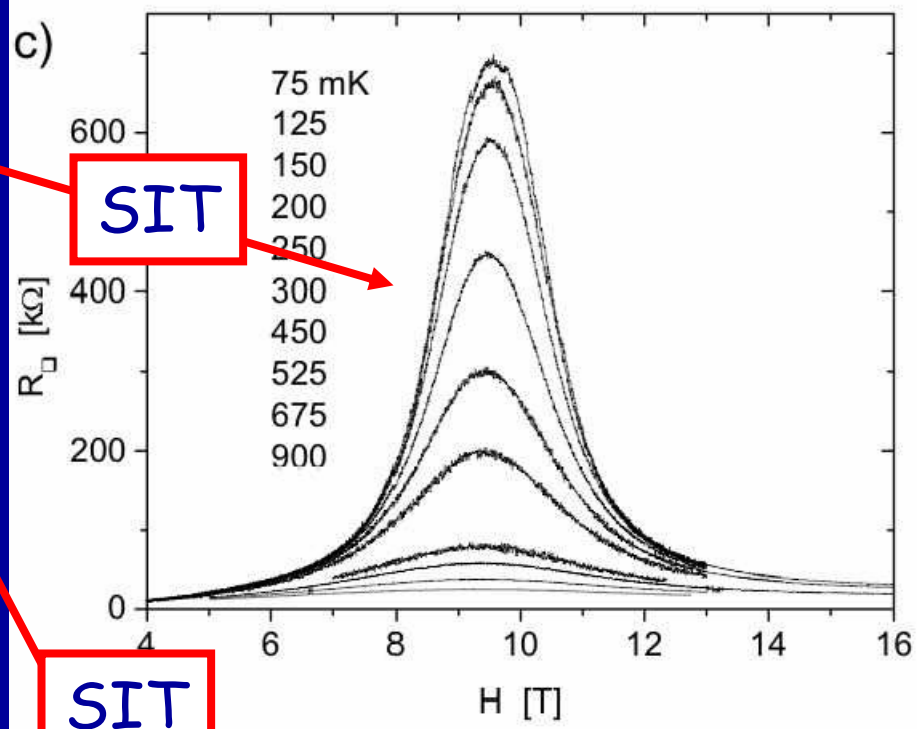

SIT

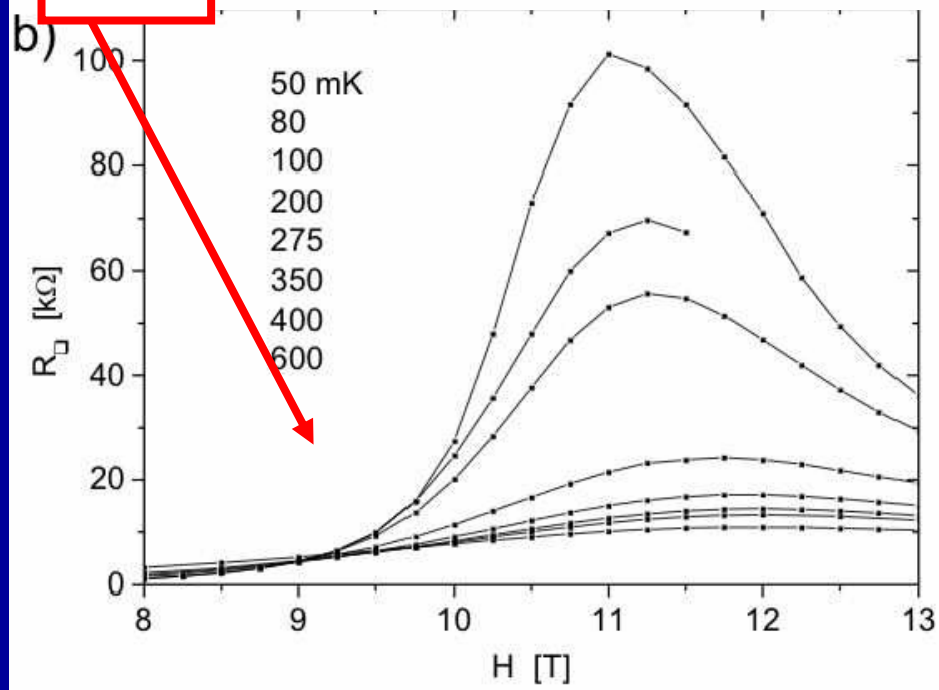

InO_x films

Myles Steiner and Aharon Kapitulnik, cond-mat/0406227

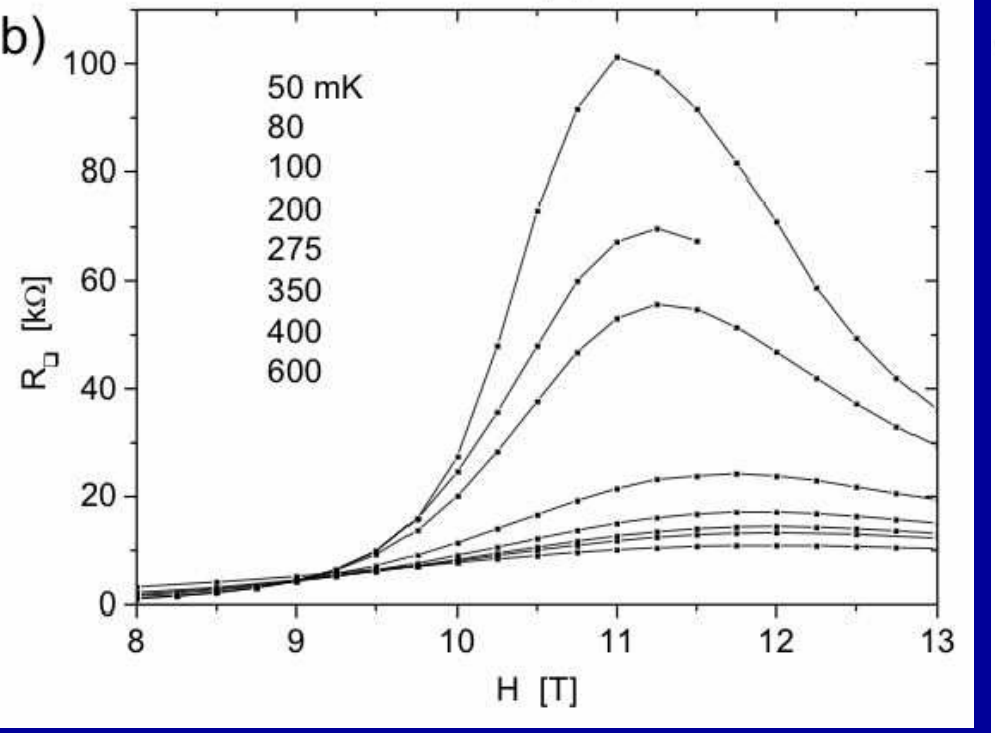

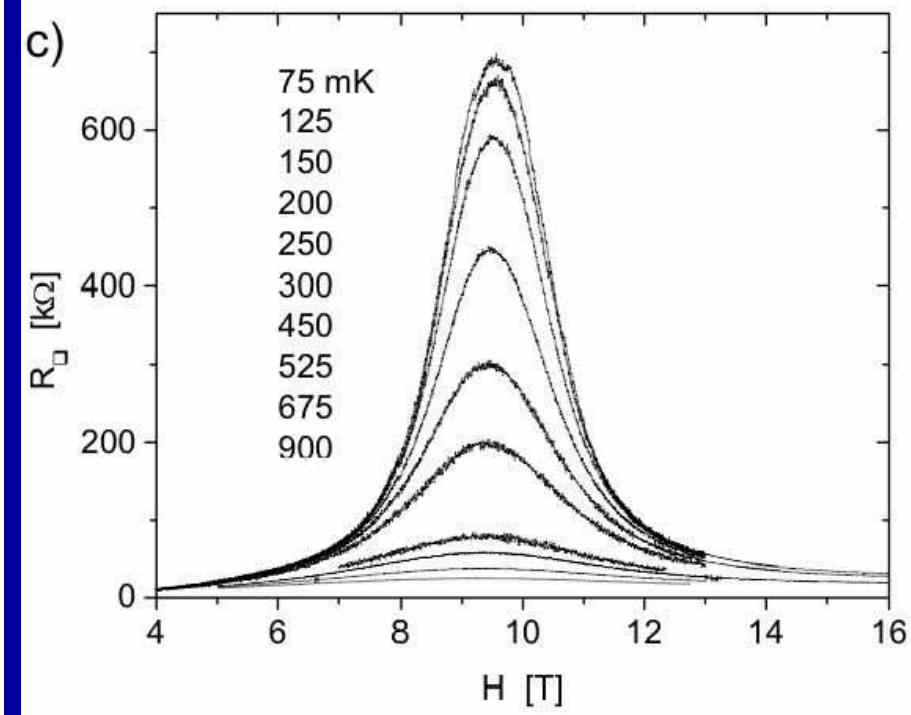

The insulating state above the crossing point becomes even more dramatic in the films with higher R_n. At low temperature and moderately high field these films reveal a new, extremely strong tendency towards the insulating phase, shown in Figures 4b and 4c. The resistance at the crossing point of both plots is comparable to that of the first film. We note, however, that the position of the crossing point shifts to lower field as the insulator strength increases. On the high field side of the peak the isotherms all decay to resistances ≤ 20 kΩ/□, above the normal resistance R_n, at the highest accessible fields.

schematic phase diagram

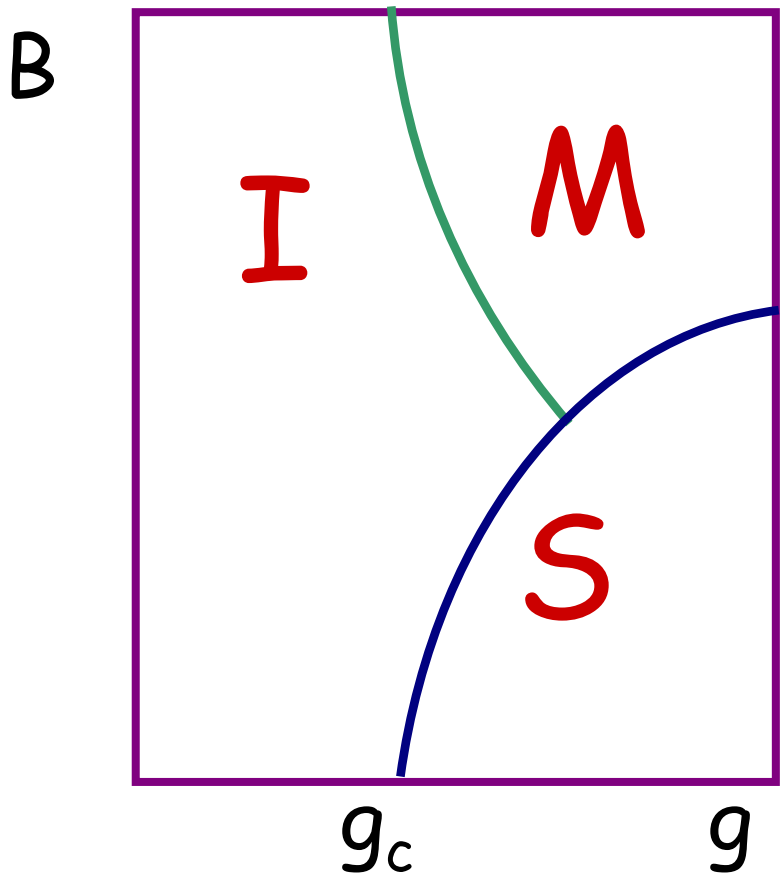

Low-Resistive Sample

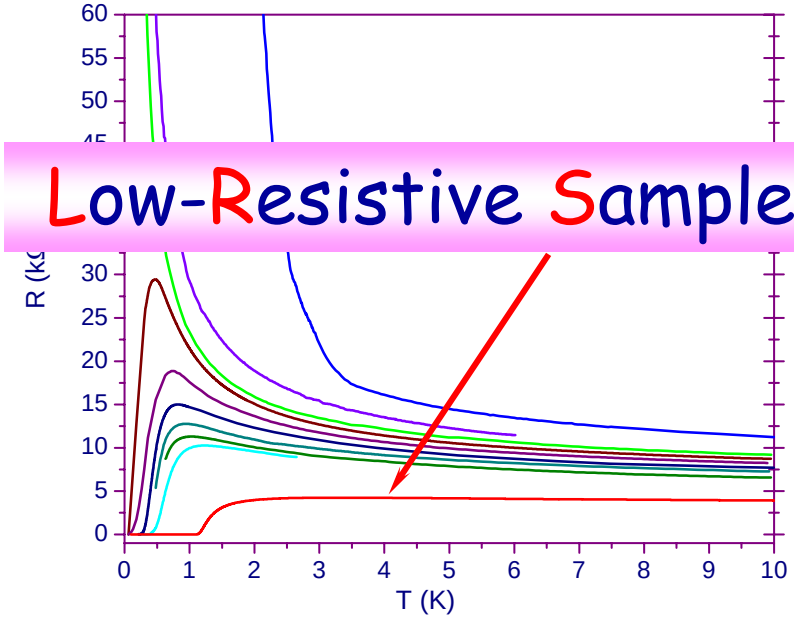

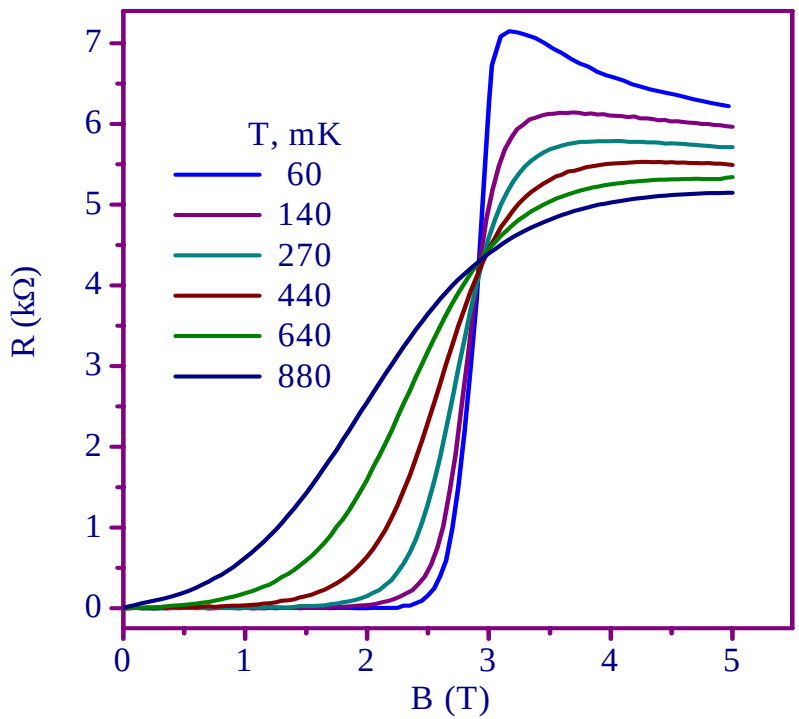

schematic phase diagram

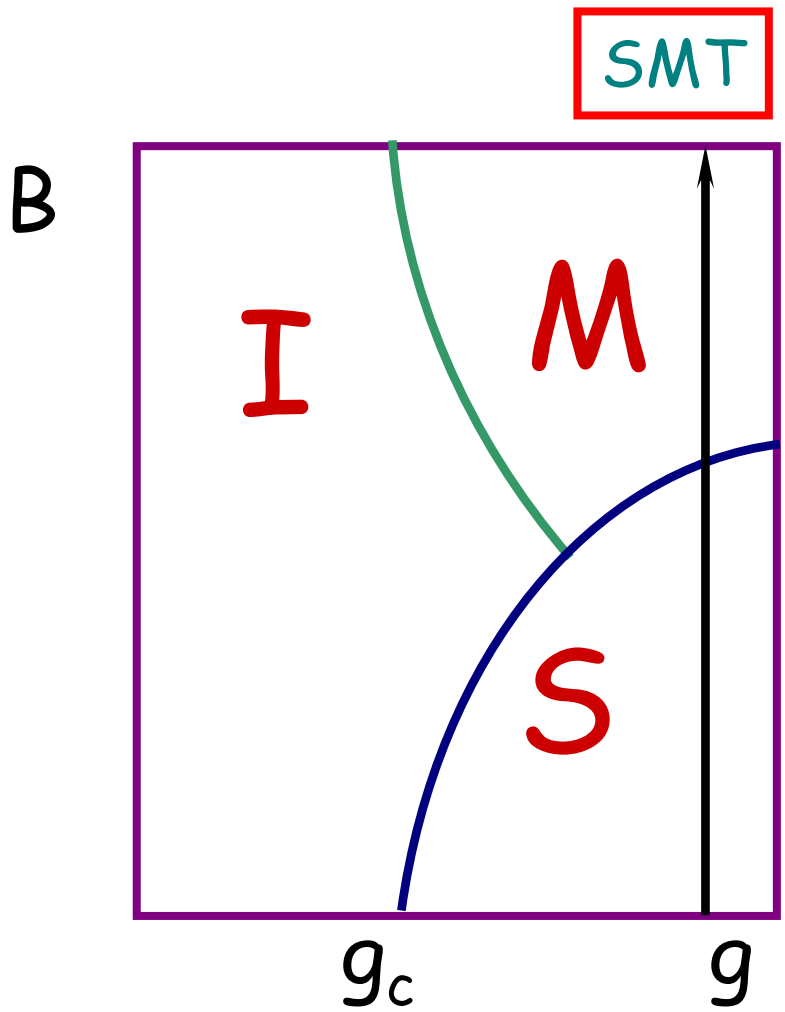

comparison with Galitski – Larkin calculations of the quantum corrections

T. Baturina, et. al., Physica B 359-361, 500 (2005)

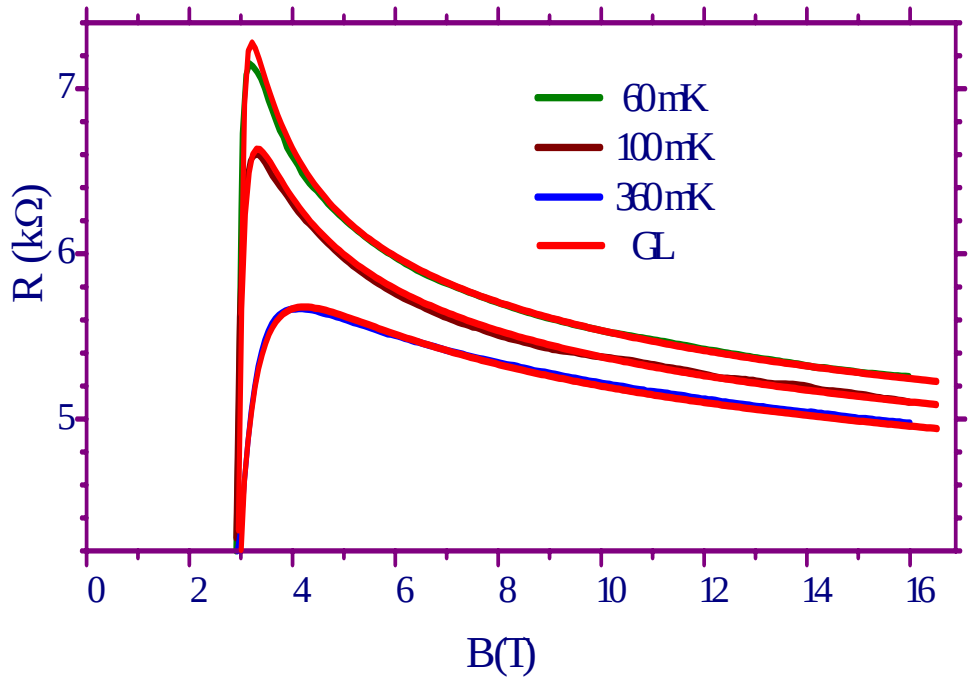

schematic phase diagram

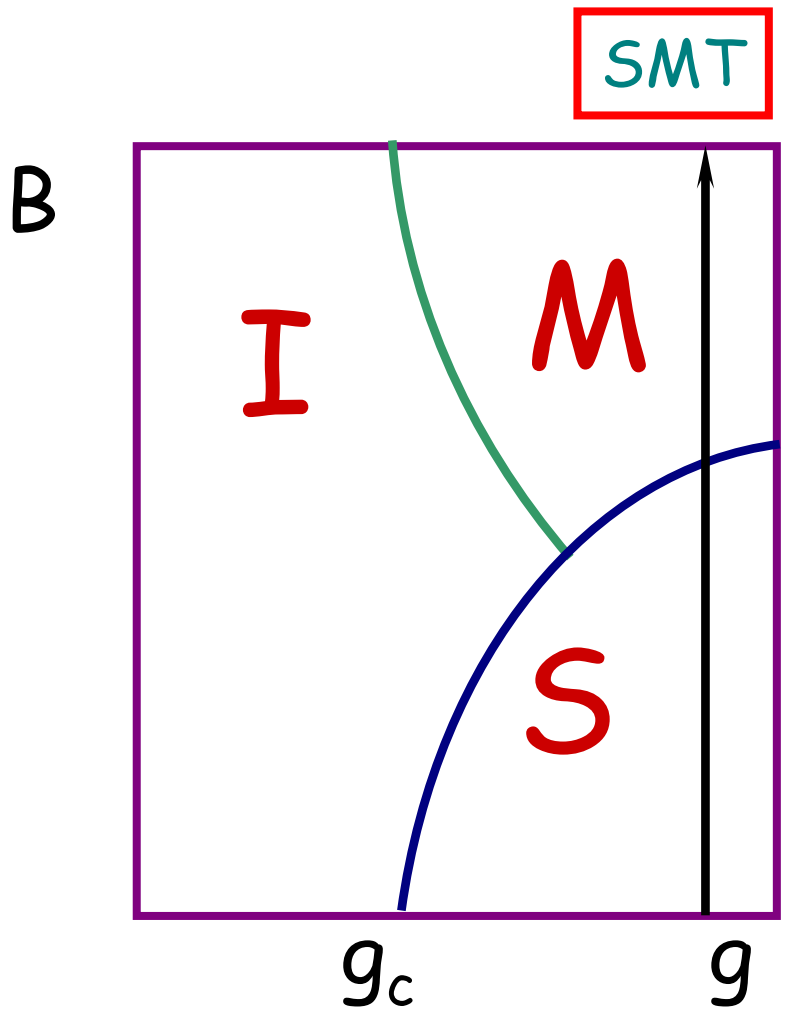

InO_x films

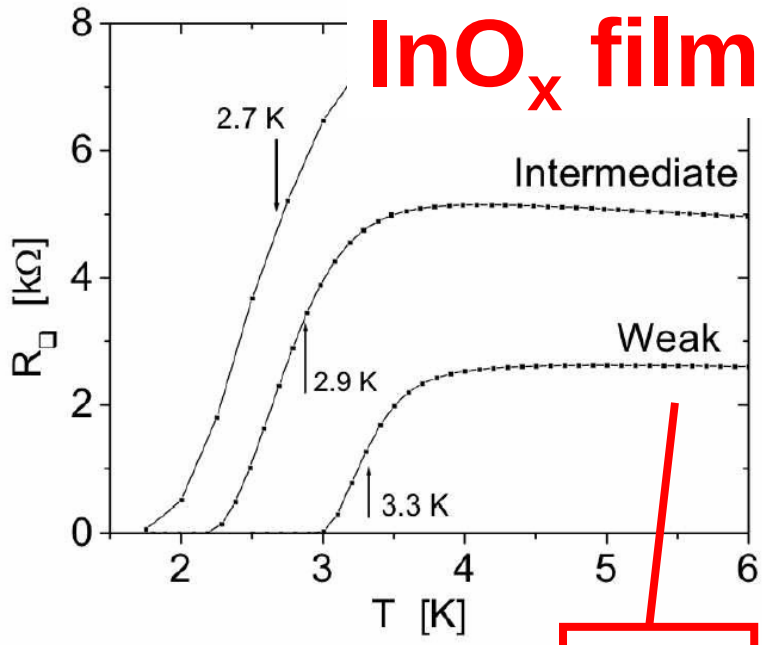

SMT

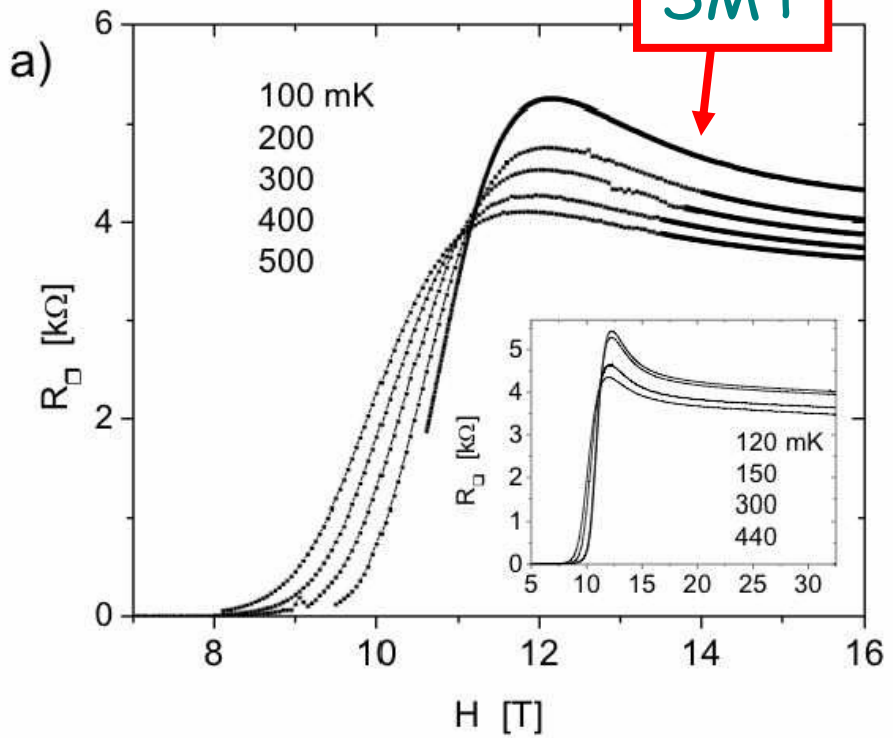

schematic phase diagram

InO_x, Be, and TiN films

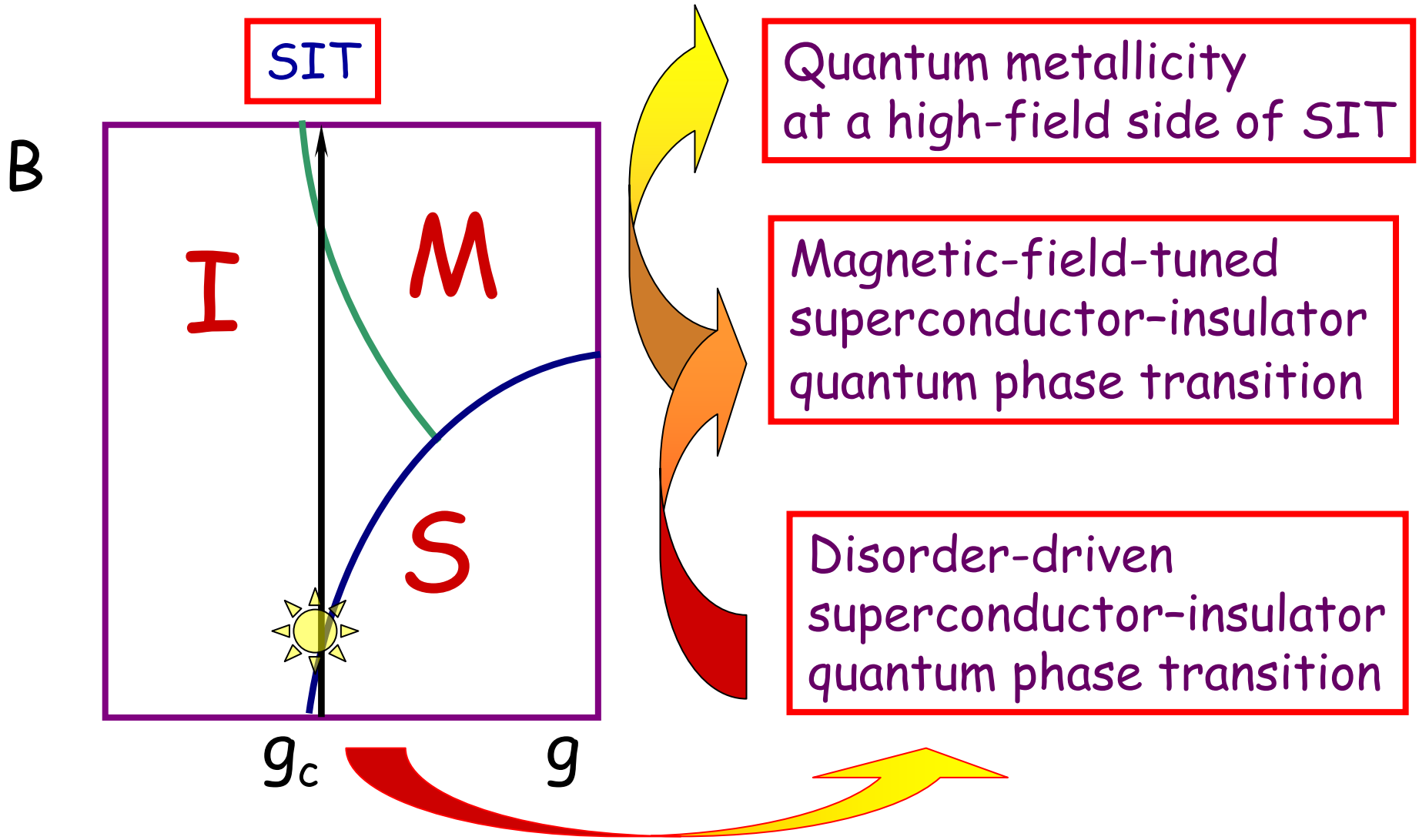

Quantum metallicity
at a high-field side of SIT

Magnetic-field-tuned
superconductor–insulator
quantum phase transition

Disorder-driven
superconductor–insulator
quantum phase transition

schematic phase diagram

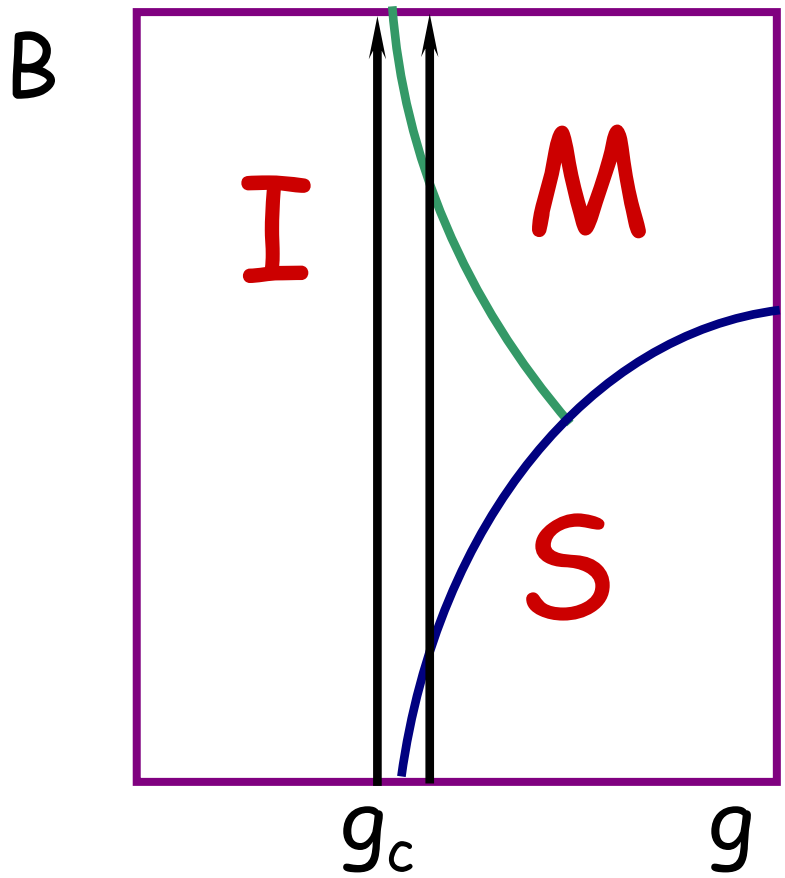

Critical Region of the Disorder-Driven Superconductor-Insulator quantum phase transition

T.I. Baturina et al., cond-mat/0705.1602

TiN films

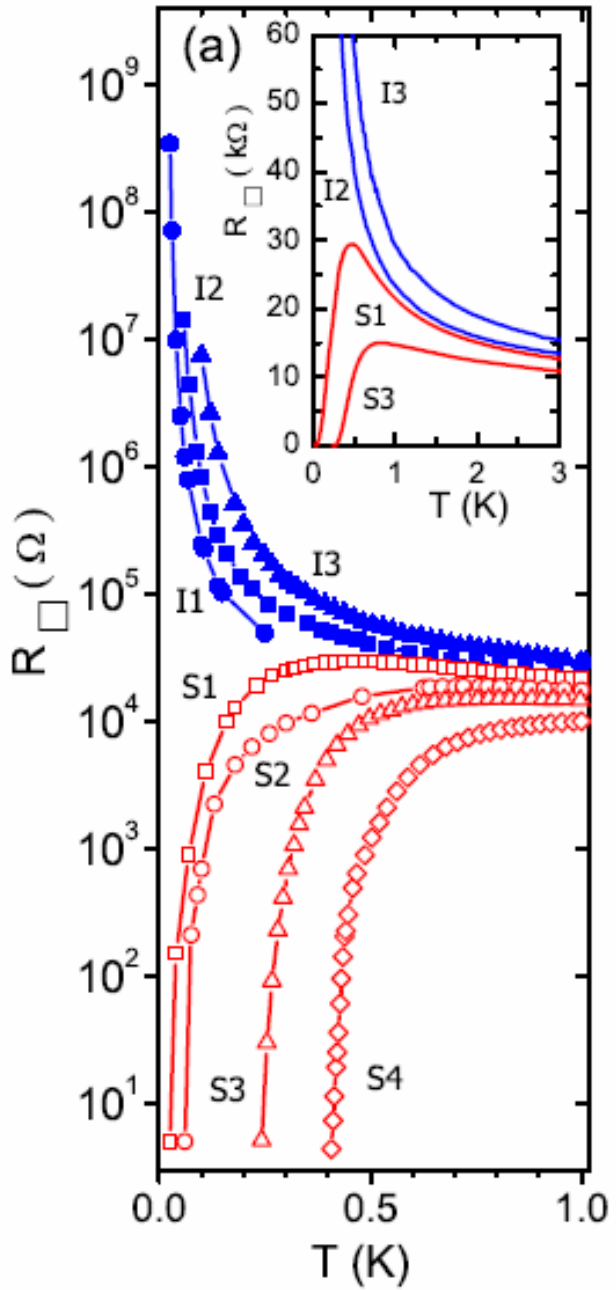

Magnetoresistance

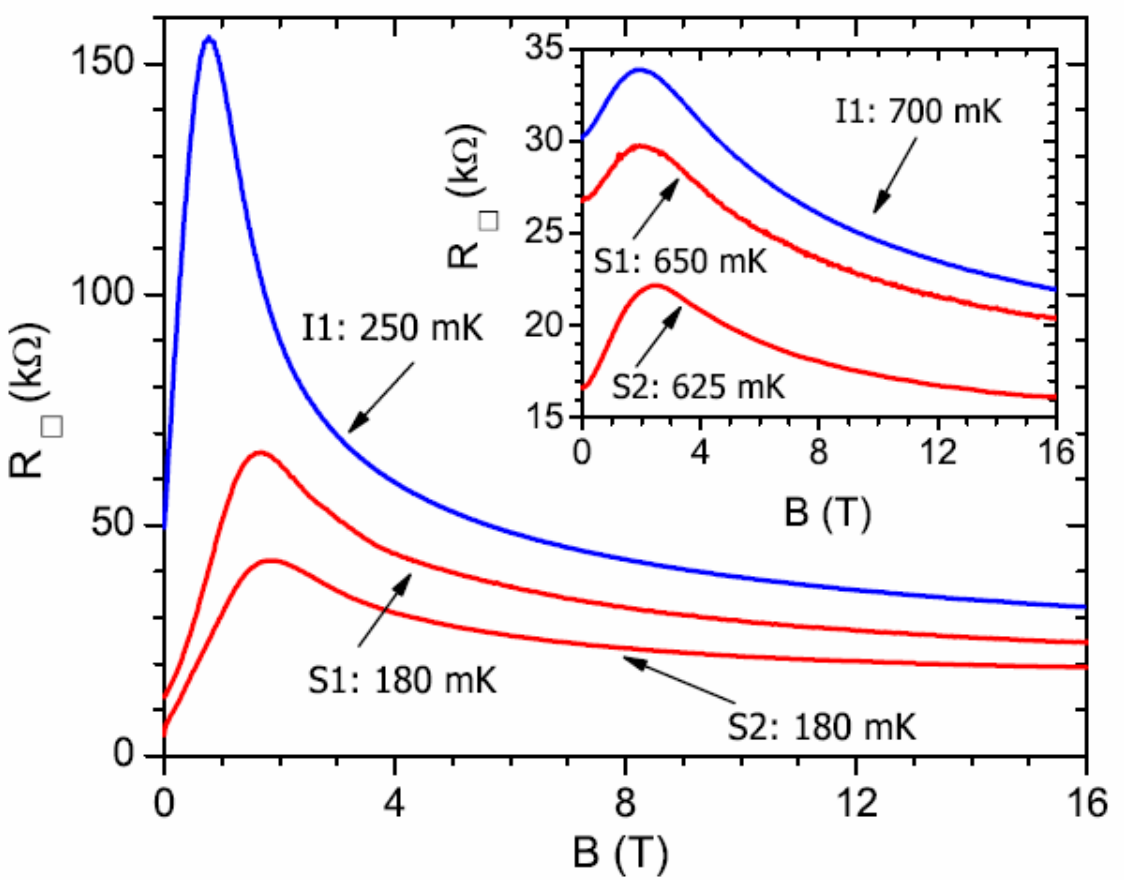

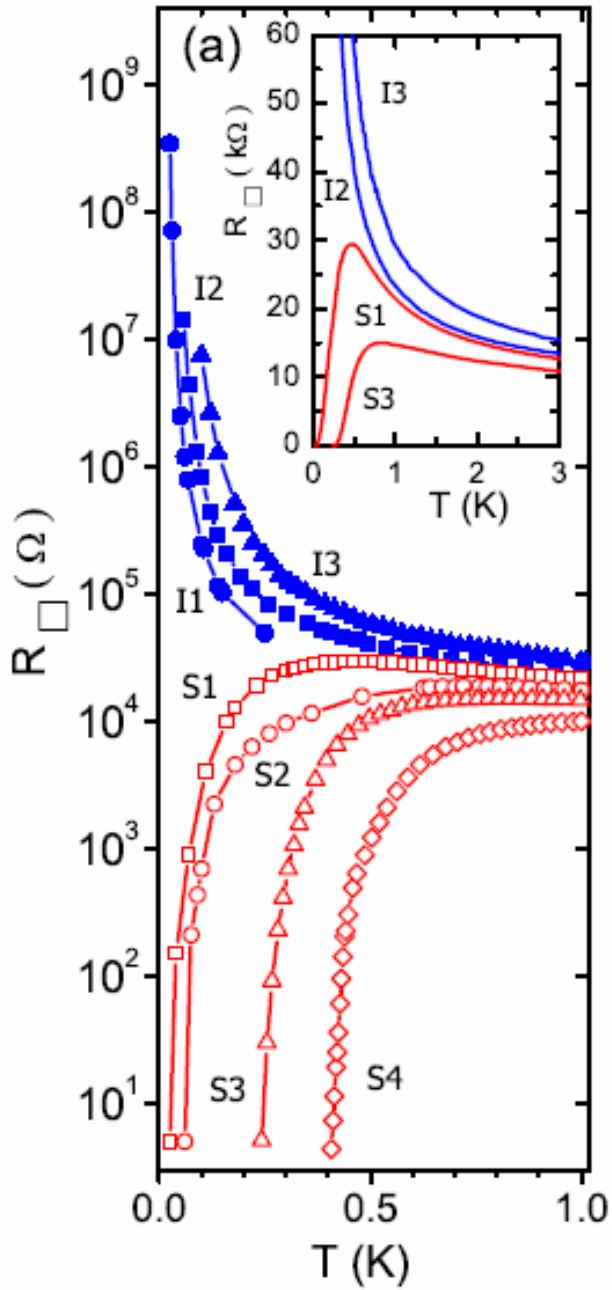

In all samples, including the insulating films, R(B) varies non-monotonously with B, starting a positive magnetoresistance (PMR) at low fields, then reaching a maximum, followed first by a rapid drop and eventually saturating at higher magnetic fields

PMR and activated behavior

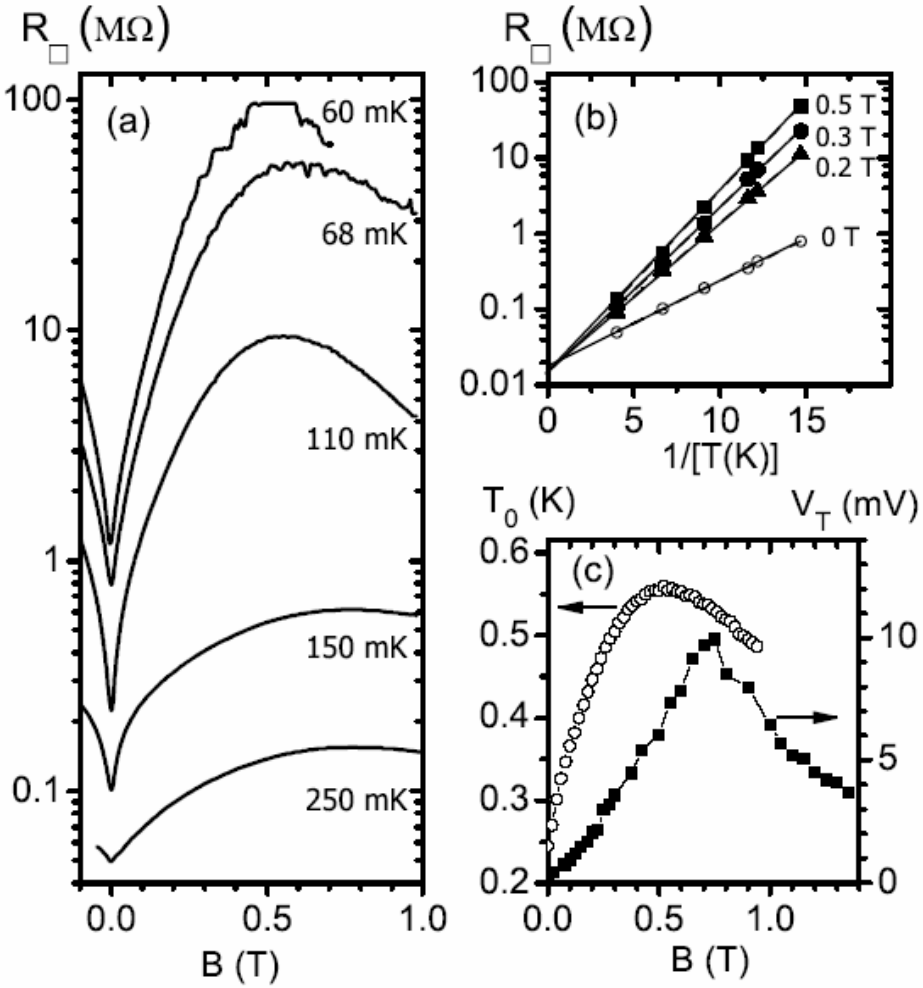

FIG. 3: (a) Sheet resistance of sample I1 as a function of the magnetic field at some temperatures listed. (b) R versus $1/T$ at $B = 0$ (open circles), 0.2 (triangles), 0.3 (filled circles), and 0.5 T (squares). The dashed lines are given by Eq. (1). (c) T_0 (left axis), calculated from fits to Eq. (1), and the threshold voltage V_T (right axis) as a function of B.

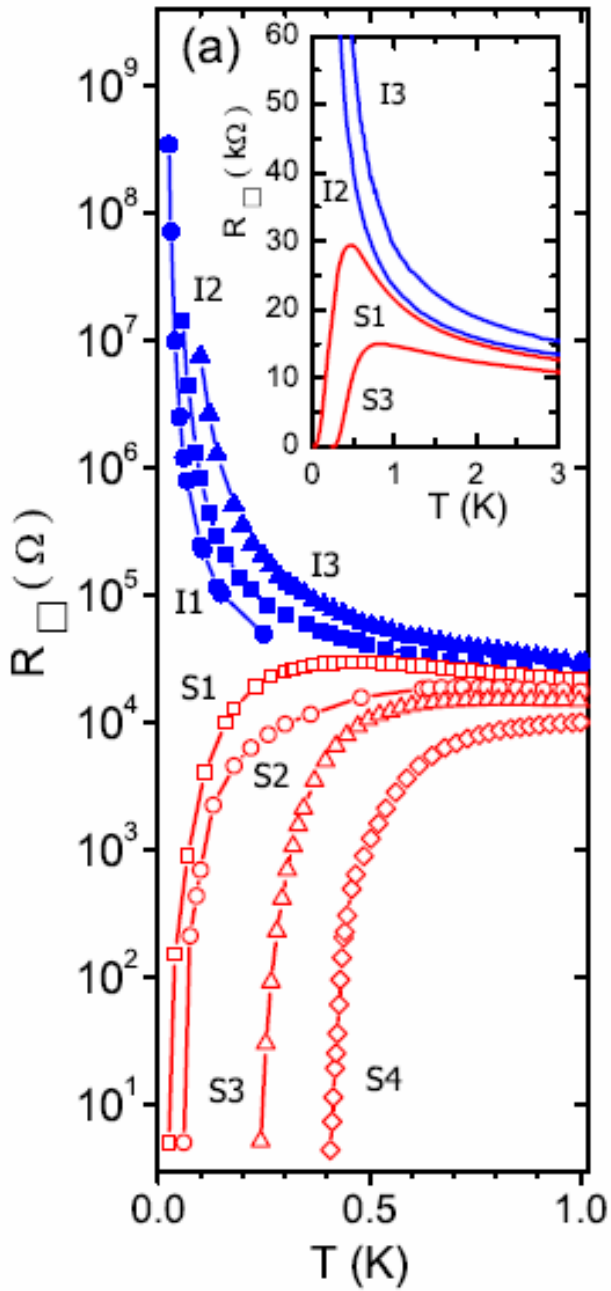

Collective insulating state: Threshold behavior of dI/dV vs V_{dc}

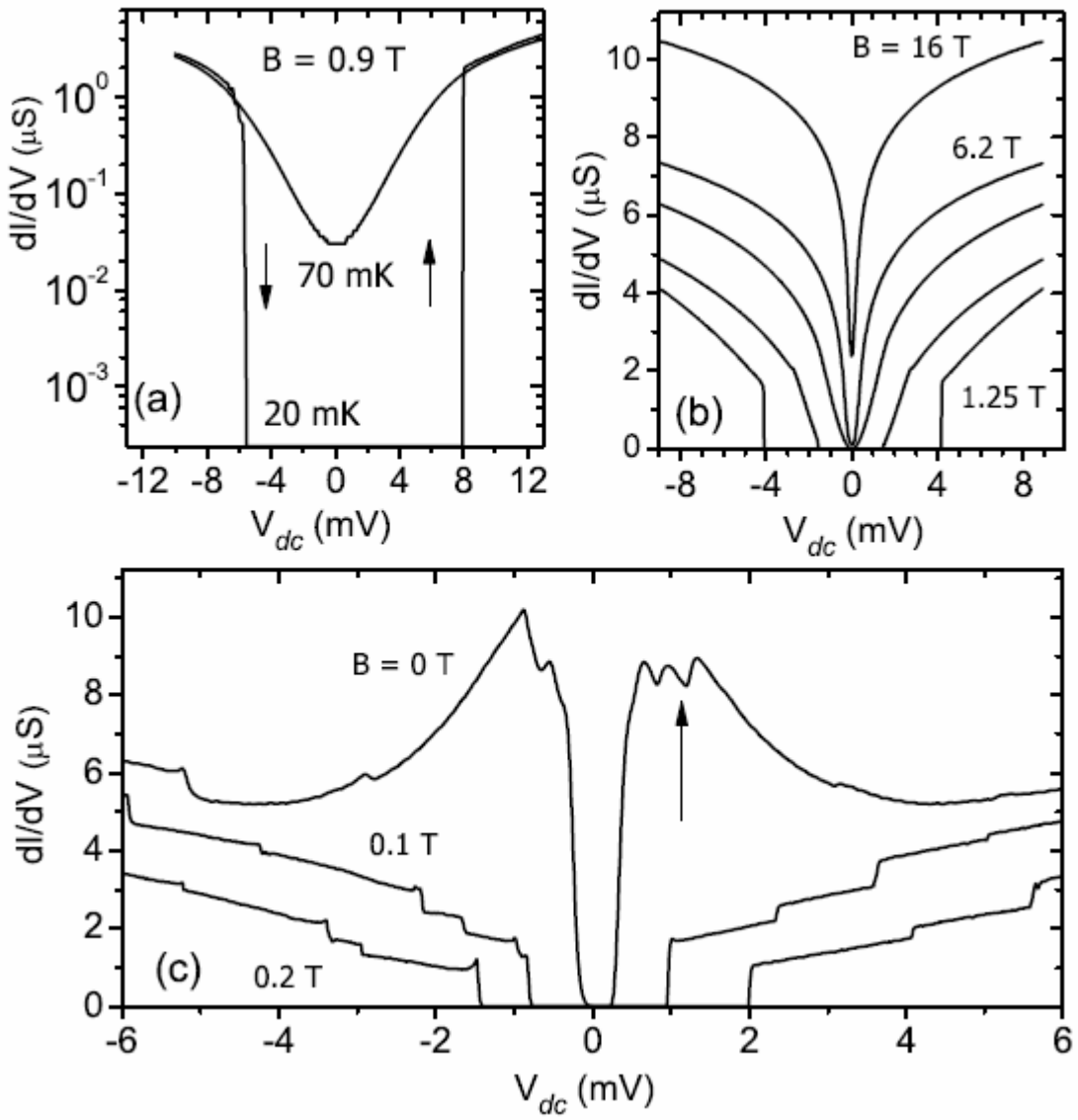

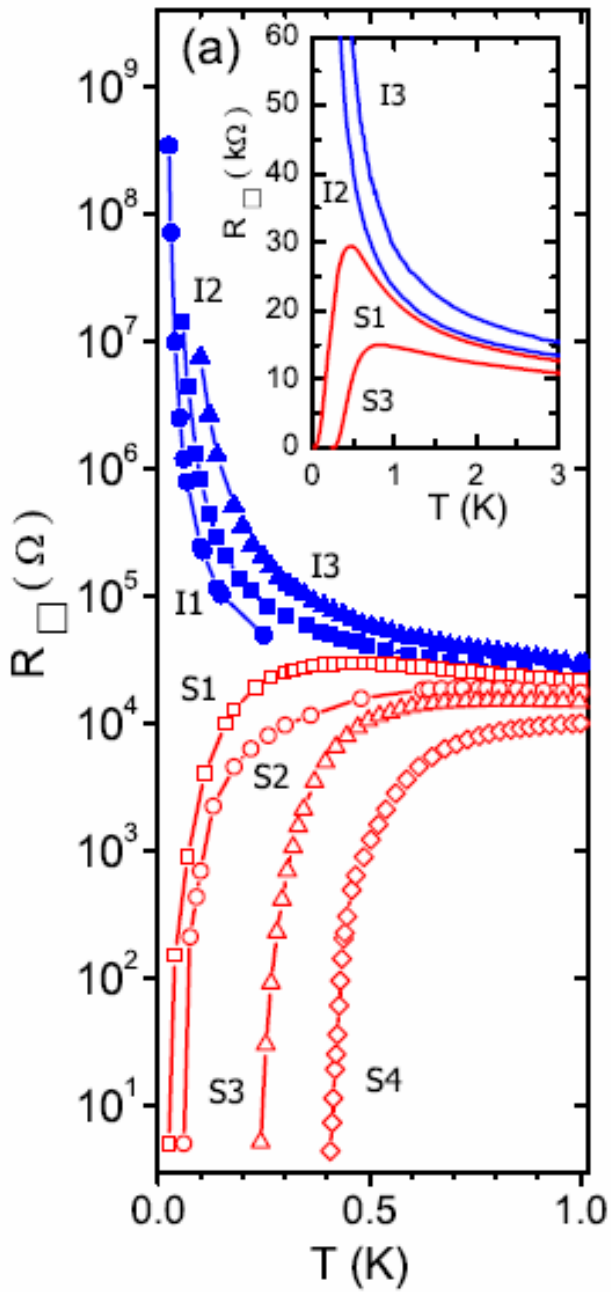

Collective insulating state: Threshold behavior of dI/dV vs V_{dc}

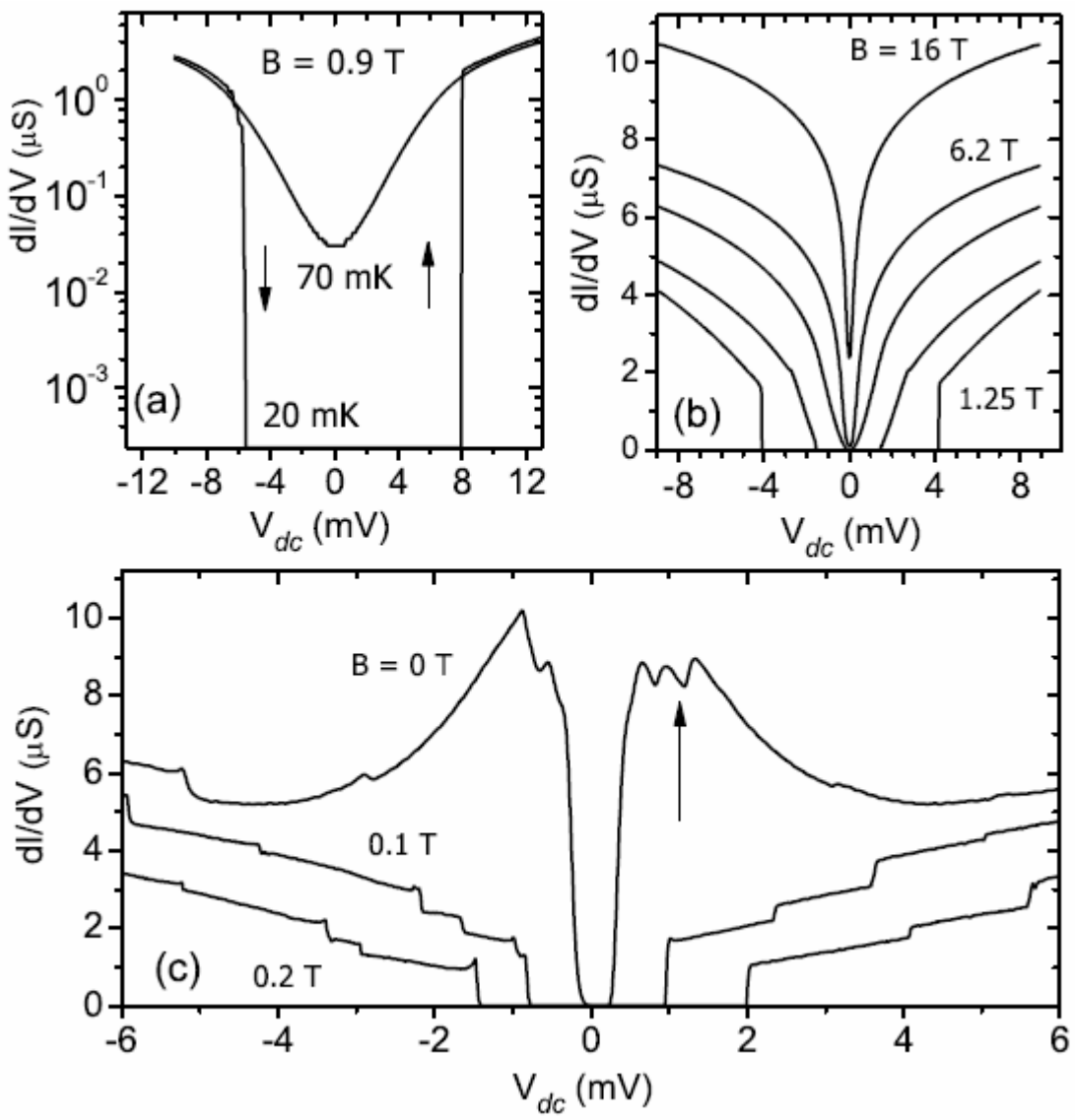

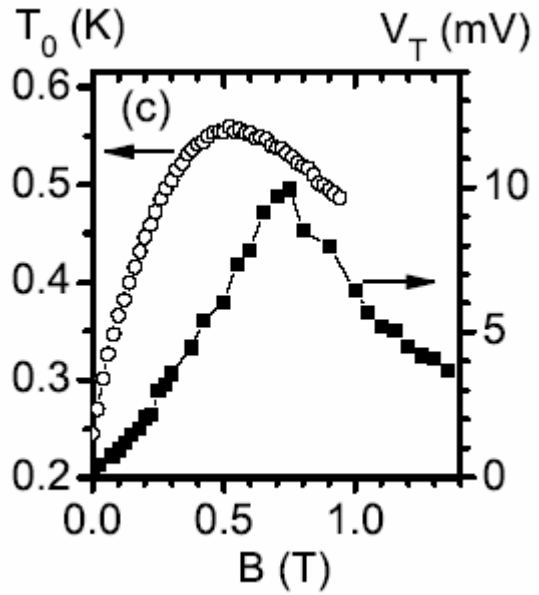

The threshold voltage changes nonmonotonically upon magnetic field

schematic phase diagram

Magnetic-field-induced insulating phase

InO_x films

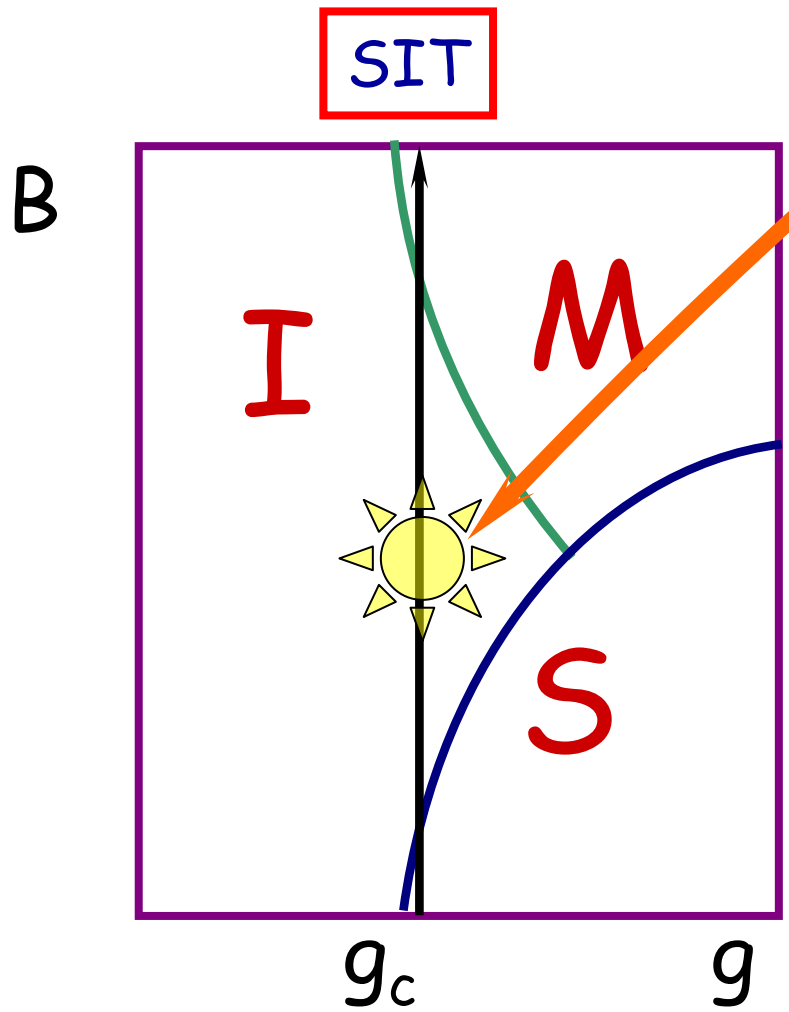

Magnetic-field-induced insulating phase

InO_x films

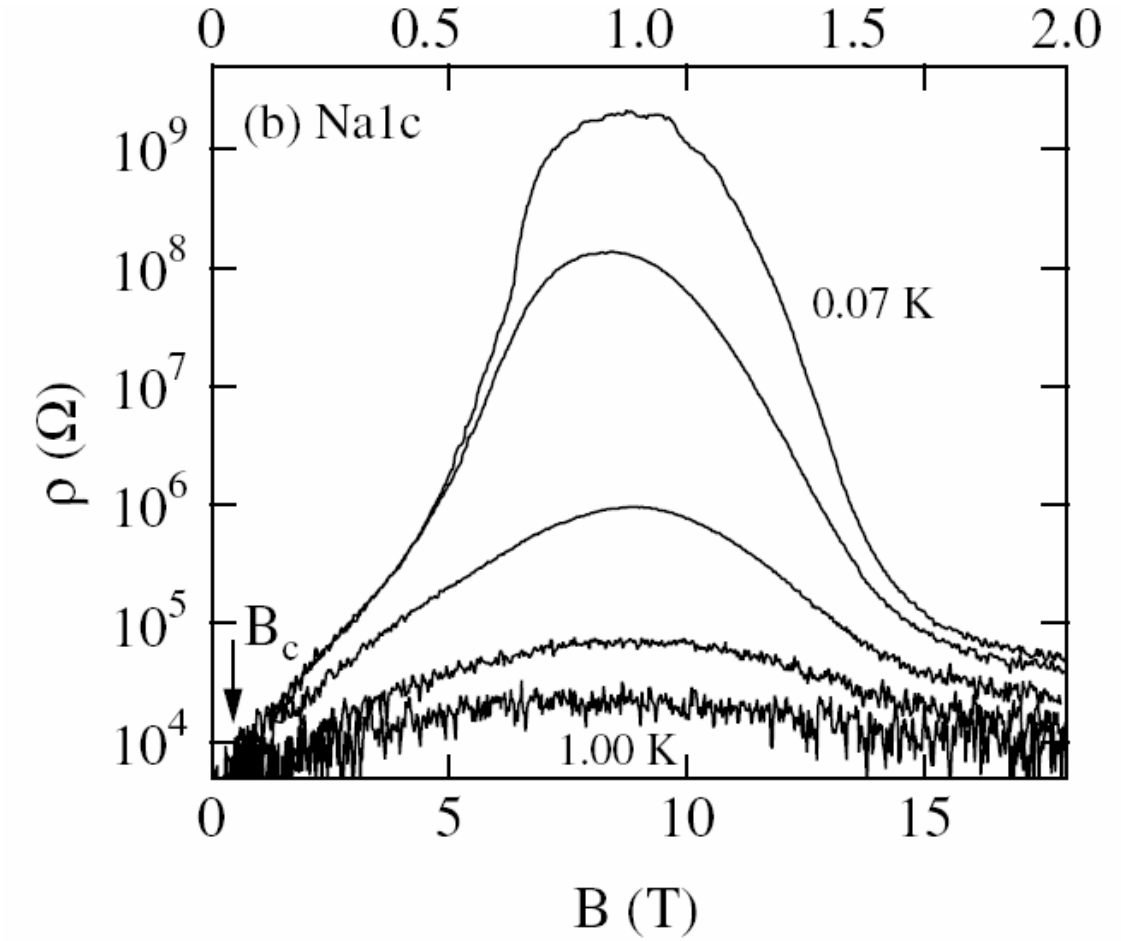

G. Sambandamurthy, L.W. Engel, A. Johansson, and D. Shahar, PRL 92, 107005 (2004).

for sample Na1c at $T = 0.07, 0.16, 0.35, 0.62$, and 1.00 K.

Magnetic-field-induced insulating phase

InO_x films

G. Sambandamurthy,
L.W. Engel,
A. Johansson,
and D. Shahar,
PRL 92, 107005 (2004).

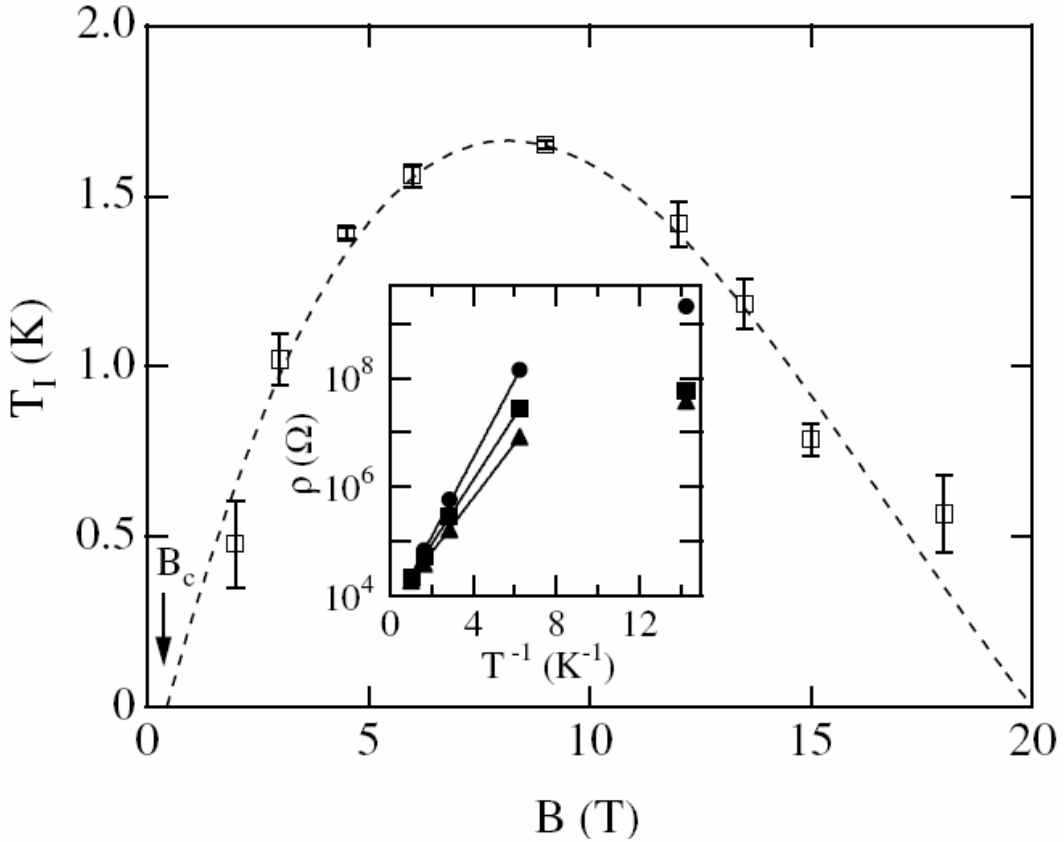

FIG. 3. Inset: ρ versus T^{-1} at $B = 6$ (squares), 9 (circles), and 12 T (triangles) for sample Na1c. The solids lines are fits to Eq. (1). The lowest T data points do not fit to the Arrhenius behavior. The main figure shows T_I, calculated from the fits to Eq. (1), as a function of B. T_I has a peak at 9 T. T_I estimates for 4 T $> B >$ 14 T suffer from large errors since the low-T ρ value is not high enough to ensure activated behavior. The vertical arrow marks B_c (= 0.45 T), where $T_I = 0$. The dashed line is a guide to the eye.

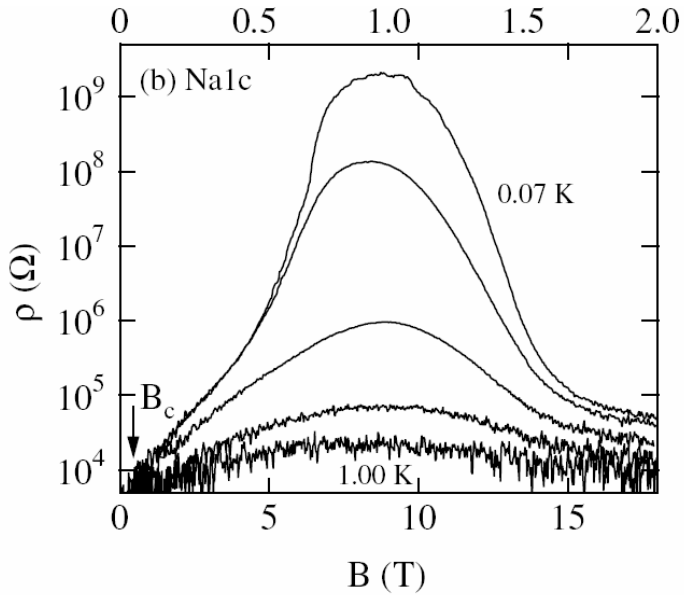

Magnetic-field-induced insulating phase

InO_x films

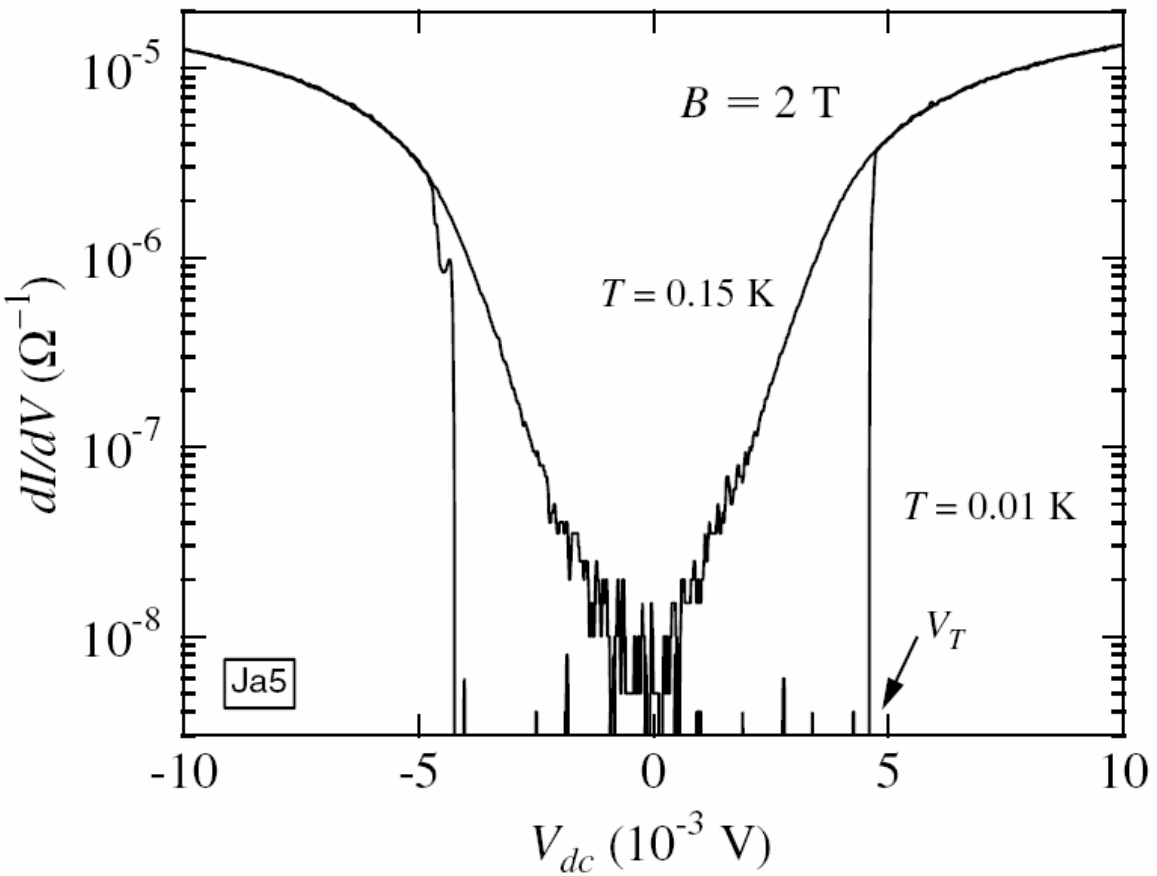

G. Sambandamurthy,
L.W. Engel,
A. Johansson,
E. Peled
and D. Shahar,
PRL 94, 017003 (2005).

Collective insulating state:
Threshold behavior
of dI/dV vs V_{dc}

FIG. 2. Comparison of the current-voltage characteristics of the B-driven insulating phase at two T's (0.15 and 0.01 K). The traces show the two-terminal differential conductance measured at $B = 2$ T as a function of dc voltage. The ac excitation voltage applied is 10 μV. The sample used is Ja5 with $B_c = 0.4$ T. V_T marks the threshold voltage for conduction at $T = 0.01$ K.

Magnetic-field-induced insulating phase

InO_x films

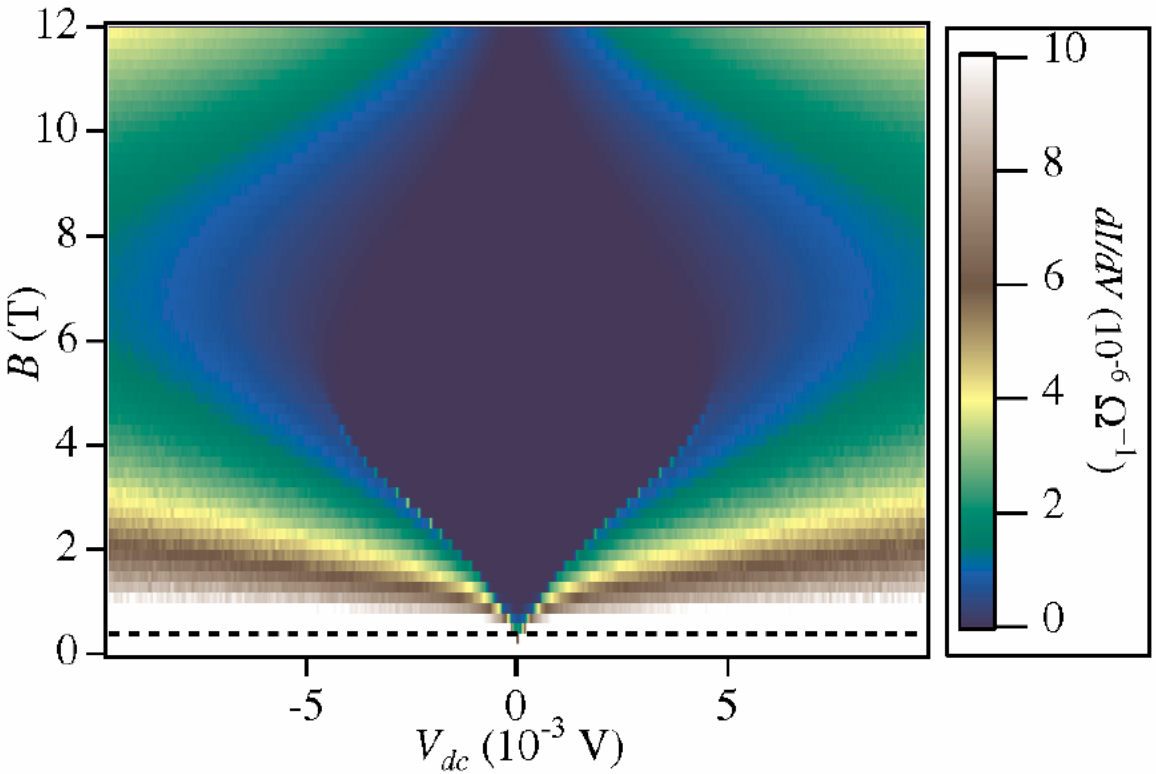

G. Sambandamurthy,
L.W. Engel,
A. Johansson,
E. Peled
and D. Shahar,
PRL 94, 017003 (2005).

Collective insulating state:
Threshold behavior
of dI/dV vs V_{dc}

FIG. 4 (color). Two-dimensional map of the dI/dV values in the $B - V_{dc}$ plane. For the sample of Fig. 2 (Ja5), we have measured dI/dV traces as a function of V_{dc} at B intervals of 0.2 T and at $T = 0.01$ K. The color scale legend on the right-hand side shows the various colors used to represent the values of dI/dV. The horizontal dashed line denotes B_c (= 0.4 T) of this sample.

InO_x film
Sc at B=0

Collective insulating state:
Threshold behavior
of dI/dV vs V_{dc}

TiN film
Ins. at B=0

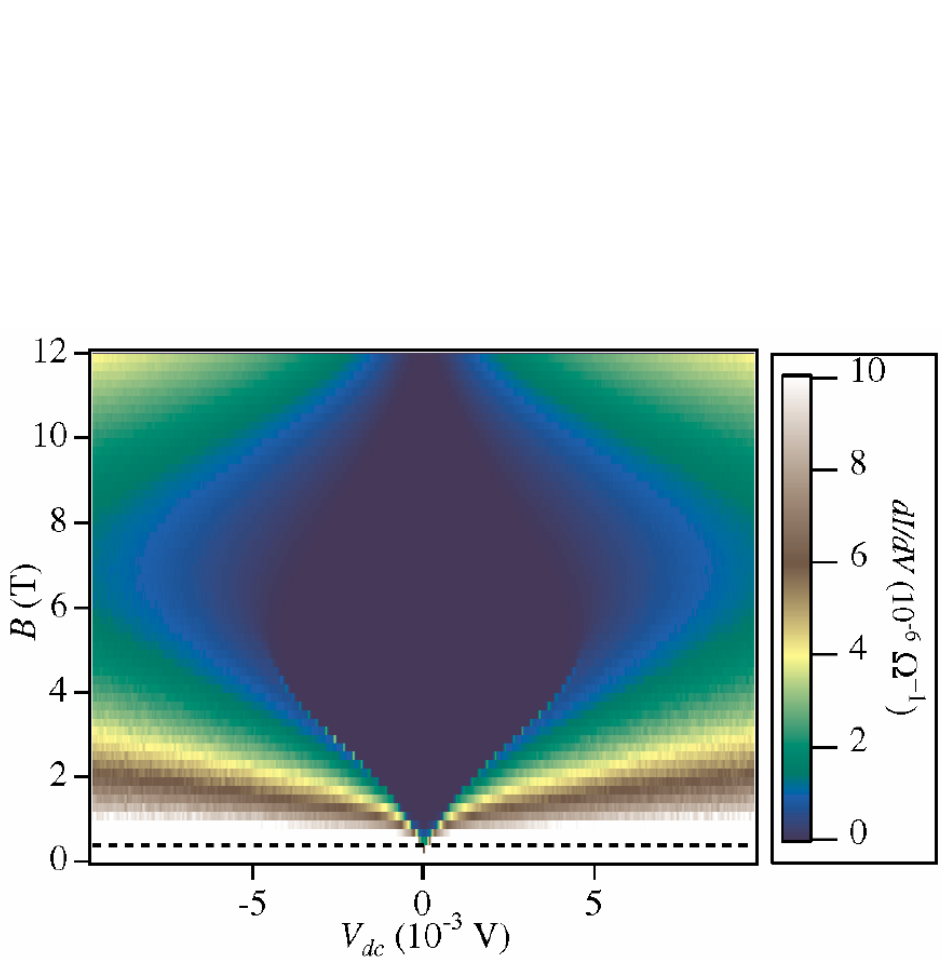

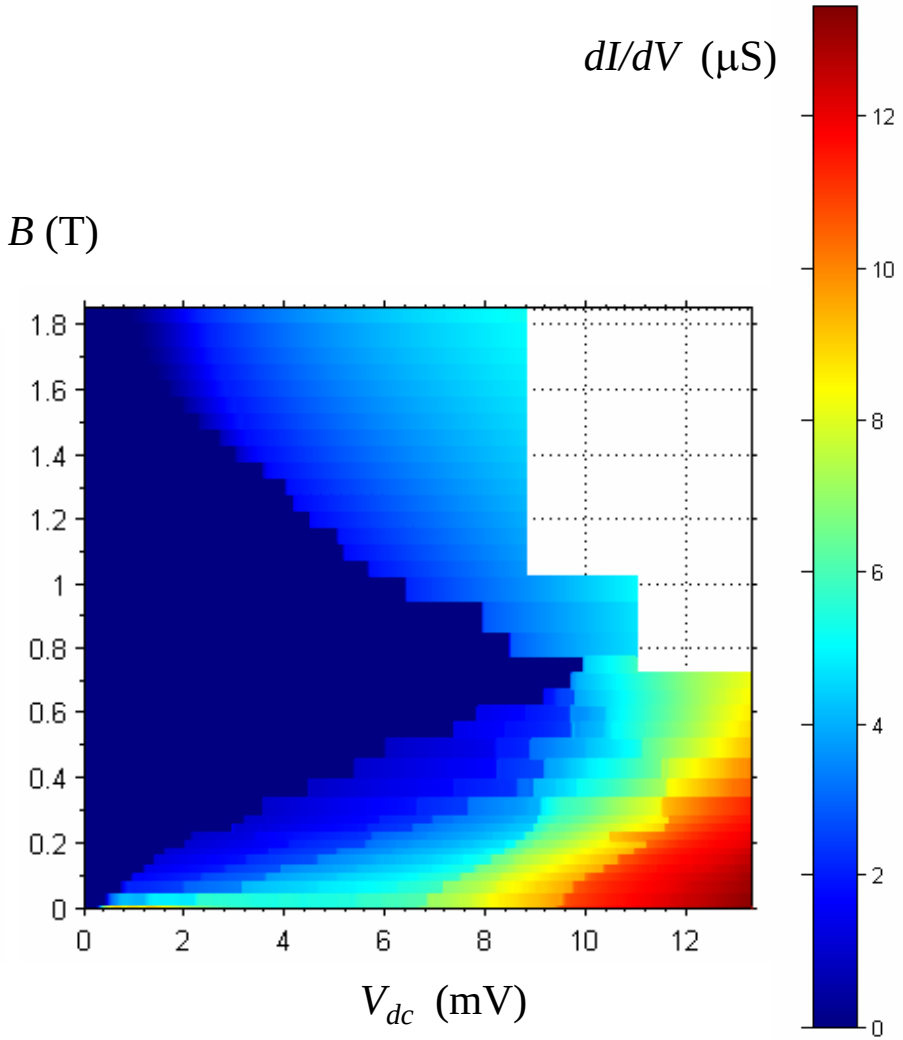

Critical Region of the Disorder-Driven Superconductor-Insulator quantum phase transition

Aggregate of Experimental Features

- ✓thermally activated behavior of the conductivity
- ✓positive magnetoresistance at low magnetic field
- ✓negative magnetoresistance with a saturation near h/e^2 in high magnetic fields
- ✓threshold behavior in the I-V characteristics

in the vicinity of the D-SIT,
the response to applied magnetic and/or electric fields, is the same irrespectively of whether the underlaying ground state is superconducting or insulating